ÇUKUROVA UNIVERSITY
INSTITUTE OF NATURAL AND APPLIED SCIENCES

MSc THESIS

Kemal AYGÜL

BUTTERFLY OPTIMIZATION ALGORITHM BASED MAXIMUM POWER POINT TRACKING OF PHOTOVOLTAIC SYSTEMS UNDER PARTIAL SHADING CONDITION

DEPARTMENT OF ELECTRICAL AND ELECTRONICS ENGINEERING

ADANA-2019

ÇUKUROVA UNIVERSITY
INSTITUTE OF NATURAL AND APPLIED SCIENCES

BUTTERFLY OPTIMIZATION ALGORITHM BASED MAXIMUM POWER POINT TRACKING OF PHOTOVOLTAIC SYSTEMS UNDER PARTIAL SHADING CONDITION

Kemal AYGÜL

MSc THESIS

DEPARTMENT OF ELECTRICAL AND ELECTRONICS ENGINEERING

We certify that the thesis titled above was reviewed and approved for the award of degree of the Master of Science by the board of jury on 17/07/2019.

…………………………………	…………………………………..	………………….……………
Prof. Dr. Mehmet TÜMAY SUPERVISOR	Asst. Prof. Dr. Tuğçe DEMİRDELEN CO-SUPERVISOR	Assoc. Prof. Dr. M. Uğraş CUMA MEMBER
………………………………….	………………………..	
Asst. Prof. Dr. M. Mustafa SAVRUN MEMBER	Asst. Prof. Dr. Adnan TAN MEMBER	

This MSc Thesis is written at the Department of Electrical and Electronics Engineering of Institute of Natural And Applied Sciences of Çukurova University.
Registration Number:

Prof. Dr. Mustafa GÖK
Director
Institute of Natural and Applied Sciences

This thesis was supported by the Scientific Research Project Unit of Cukurova University with a project number of FYL-2018-10587.

ABSTRACT

MSc THESIS

BUTTERFLY OPTIMIZATION ALGORITHM BASED MAXIMUM POWER POINT TRACKING OF PHOTOVOLTAIC SYSTEMS UNDER PARTIAL SHADING CONDITION

Kemal AYGÜL

ÇUKUROVA UNIVERSITY
INSTITUTE OF NATURAL AND APPLIED SCIENCES
DEPARTMENT OF ELECTRICAL AND ELECTRONICS ENGINEERING

Supervisor : Prof. Dr. Mehmet TÜMAY
Year: 2019, Pages: 81
Jury : Prof. Dr. Mehmet TÜMAY
: Asst. Prof. Dr. Tuğçe DEMİRDELEN
: Assoc. Prof. Dr. M. Uğraş CUMA
: Asst. Prof. Dr. Adnan TAN
: Asst. Prof. Dr. M. Mustafa SAVRUN

In the recent literature many soft computing techniques implemented for the MPPT of PV systems under PSC such as gray wolf optimization (GWO), particle swarm optimization (PSO) and Gravitational Search Algorithm (GSA). However, the performance of the MPP trackers still needs to be improved. The aim of this thesis is to implement a new global optimization algorithm for the MPPT of PV systems under PSC to improve the performance. For this purpose, a PV system is modelled in MATLAB/Simulink. Butterfly optimization algorithm (BOA) is implemented for three insolation scenarios on the modelled system. The results of the BOA is compared with the results of the PSO-GSA and GWO algorithm. The results showed that the BOA method is able to give high accuracy of tracking the GMPP and better speed than PSO-GSA and GWO methods.

Keywords: Partial Shading, Photovoltaic, Solar Energy, Butterfly Optimization Algorithm, MPPT

ÖZ

YÜKSEK LİSANS TEZİ

KISMİ GÖLGELENME DURUMUNDA FOTOVOLTAİK SİSTEMLERİNİN KELEBEK OPTİMİZASYON ALGORİTMASI TABANLI MAKSİMUM GÜÇ NOKTASI TAKİBİ

Kemal AYGÜL

ÇUKUROVA ÜNİVERSİTESİ
FEN BİLİMLERİ ENSTİTÜSÜ
ELEKTRİK - ELEKTRONİK MÜHENDİSLİĞİ ANABİLİM DALI

Danışman : Prof. Dr. Mehmet TÜMAY
Yıl: 2019, Sayfa: 81
Jüri : Prof. Dr. Mehmet TÜMAY
: Dr.Öğr. Üyesi Tuğçe DEMİRDELEN
: Doç. Dr. Mehmet Uğraş CUMA
: Dr.Öğr. Üyesi Adnan TAN
: Dr.Öğr. Üyesi M. Mustafa SAVRUN

Literatürde kısmi gölgelenme altındaki PV sistemlerinin maksimum güç noktası takibi (MPPT) için Gri kurt eniyileme (GWO), parçacık sürü eniyileme (PSO) ve Gravitasyonel Arama Algoritması (GSA) gibi birçok esnek hesaplama yöntemi uygulanmıştır. Bununla birlikte, MPP izleyicilerinin performansının hala iyileştirilmesi gerekmektedir. Bu tezin amacı, kısmi gölgelenme altındaki PV sistemlerinin MPPT'si için sistemin performansını artıracak yeni bir global eniyileme algoritması uygulamaktır. Bu amaçla bir PV sistemi modellenmiştir. Kelebek optimizasyon algoritması (BOA), modellenen sistemde üç ayrı güneşlenme senaryosu için uygulanmıştır. BOA'nın sonuçları, PSO-GSA ve GWO algoritmalarının sonuçlarıyla karşılaştırılmıştır. Sonuçlar, BOA yönteminin GMPP izlemede yüksek doğruluk ve PSO-GSA ve GWO yöntemlerinden daha yüksek hız sağlayabildiğini göstermiştir.

Anahtar Kelimeler: Kısmi Gölgelenme, Fotovoltaik, Güneş Enerjisi, Kelebek Optimizasyon Algoritması, MPPT

EXTENDED SUMMARY

Due to the increasing energy demand with the increase of the industrialization and the depletion of fossil fuels, the need for an alternative and sustainable energy source has emerged. Among the alternatives, solar energy is the most promising one due to its availability all around the world. There are a few ways to use solar energy, but the most popular way is to use photovoltaic (PV) cells in order to generate electricity by using the energy of photons in the sunlight.

Current and Voltage ratings of a PV cell is not appropriate to use it alone for most of the applications. The typical open circuit voltage of a PV cell is around 0.6 V that is much lower than the rated voltage of most electrical systems. To increase the voltage level, many PV cells is connected series. For example, PV modules with 36 series connected PV cells are manufactured for 12 V battery applications. The module has open circuit voltage around 21 V and maximum power point voltage around 17 V that is suitable for charging 12 V batteries under ordinary insolation conditions. Similar to the series connection, PV cells are connected parallel to increase the rated current of a module. As the power rating of the application increases such as grid-connected applications, the number of series and parallel connected cells in a module are also increase. Just like PV cells, the same parameters are valid for PV modules. PV modules are connected in series and parallel combinations to increase the current and voltage ratings and formed PV arrays.

During the manufacturing process, the PV cells are connected series and parallel based on the assumption that all cells have identical characteristics. But in practice when some of the parameters of one or more of the cells in the string differ from others, there will be an electrical loss called mismatch loss. Mismatch conditions occur due to reasons such as broken glass cover, flaws caused by the manufacturing process and environmental effects such as partial shading.

Usually, mismatched parameters are open circuit voltage and short circuit current. When PV cells are connected in series the crucial parameter is short circuit current. and when PV cells are connected in parallel the crucial parameter is open circuit voltage. Mismatch losses caused by manufacturing process are usually small losses and compensated by manufacturing tolerances. But mismatch losses caused by shading are usually major losses.

When a PV cell does not receive sunlight due to shading of clouds, trees, buildings, etc. it is called a bad cell. If one cell in the string unable to generate current i.e. become a bad cell, it will be forced to operate in the reverse bias region by other cells. This means the bad cell will act as a load to other cells and start to dissipate heat. This condition may cause the breakdown of the p-n junction, melting of the solder in the PV module and harm to the covering material. This condition is called the hot spot on the PV module. In order to prevent the hot spot condition, additional diodes called bypass diodes are used in the string. The purpose of using bypass diodes in the PV string is to restrict the reverse bias voltage on the PV cell and prevent it to reach the breakdown voltage.

Under uniform insolation, the power-voltage characteristic of the PV system has only one maximum power point. But because of dust, trees, high buildings in the surrounding area, partial shading conditions (PSC) occur in photovoltaic (PV) systems. When this condition occurs the power-voltage curve of the PV system has multiple peaks because of the by-pass diodes. These peak points are called the global maximum power point (GMPP) and local maximum power points (LMPP). This condition makes the maximum power point tracking (MPPT) procedure a challenging task

There are some main drawbacks of photovoltaic systems; efficiency and high initial cost. Because of this condition, it is necessary to operate PV systems at their maximum efficiency. This condition increased the importance of maximum power point tracking (MPPT). Maximum power point tracking (MPPT) is a process of obtaining the maximum power from the PV module fulfilled by MPPT converters. The term MPPT converter comprises the MPPT algorithm, the controller of the power converter and the power converter. Different types of MPPT methods have been proposed to the literature during recent years. This includes Particle Swarm Optimization, Grey Wolf Optimization, ANN-based methods, Flower Pollination Algorithm and more.

The task of the MPPT algorithm is to find the maximum power point of the PV system. The control parameters of the MPPT algorithm are mostly duty cycle and voltage. In the case of the duty cycle, the MPPT algorithm controls the PWM signal of the power converter. However, in the voltage case, the MPPT algorithm gives a reference voltage to the controller of the power converter. The controller of the power converter may be a PI controller or the Fuzzy logic controller. The most common power converters for the MPPT system in the literature are a boost converter, buck converter, buck-boost converter, and SEPIC converter.

The power converter used for the MPPT mostly connected to the output of the PV system and driven by a PWM signal. The main parameters in the design of the power converters are inductance and capacitance. The inductance affects the operation mode of the converter. If the inductance is chosen too small then the converter will operate in the discontinuous current mode that makes the output unstable. If the inductance is chosen too large, then the converter will have a slow transient response. The capacitance affects the voltage ripples and needs to be calculated in order to maintain the desired ripple percentage. If the capacitance is chosen too small then the ripple voltage will be too large. If the capacitor is chosen too large then the converter will have a slow transient response.

The main contribution of this paper is improving the tracking speed by implementing BOA to the MPPT of the PV system under PSC. Thus, in real time applications a promising alternative presented to the literature to improve the performance of the PV systems under variable PSC because of its fast-tracking speed. PV system consists of PV array, boost converter and load are modeled and simulated in MATLAB/Simulink. BOA algorithm is implemented for three different insolation scenarios on the PV array. The results of the BOA algorithm verified by a comparative analysis with PSO-GSA and GWO algorithms. The results show that BOA can give high accuracy and better tracking speed than these algorithms in recent literature.

GENİŞLETİLMİŞ ÖZET

Sanayileşmenin artmasıyla birlikte artan enerji talebinden ve fosil yakıtların tükenmesinden dolayı, alternatif ve sürdürülebilir bir enerji kaynağına ihtiyaç duyulmaktadır. Alternatifler arasında, güneş enerjisi tüm dünyadaki bulunabilirliğinden dolayı en çok öne çıkandır. Güneş enerjisini kullanmanın birkaç yolu vardır, ancak en popüler yöntem güneş ışığındaki fotonların enerjisini kullanarak elektrik üretmek için fotovoltaik (PV) hücreleri kullanmaktır.

Bir PV hücresinin akım ve gerilim değerleri uygulama alanlarının çoğu için tek başına kullanılmaya uygun değildir. PV hücrenin açık devre gerilimi, çoğu elektrik sisteminin nominal gerilimi çok daha düşük olan 0.6 V civarındadır. Gerilim seviyesini arttırmak için birçok PV hücresi seri bağlanır. Örneğin, 36 seri bağlı PV hücreli PV modülleri, 12 V akü uygulamaları için üretilmiştir. Modül, 21 V civarında açık devre gerilimine ve 17 V civarında maksimum güç noktası gerilimine sahiptir; bu, normal güneşlenme koşullarında 12 V pilleri şarj etmek için uygundur. Seri bağlantıya benzer şekilde, PV hücreler bir modülün nominal akımını artırmak için paralel bağlanır. Uygulamanın güç seviyesi arttıkça, bir modüldeki seri ve paralel bağlı hücrelerin sayısı da artar. PV hücreler gibi, aynı parametreler PV modüller için de geçerlidir. PV modüller, akım ve gerilim değerlerini ve oluşan PV dizilerini artırmak için seri ve paralel kombinasyonlarda bağlanır.

Üretim işlemi sırasında, PV hücreler tüm hücrelerin aynı özelliklere sahip olduğu varsayımına dayanarak seri ve paralel bağlanır. Fakat pratikte, dizideki hücrelerin bir veya daha fazlasının bazı parametrelerinin diğerlerinden farklı olduğu durumlarda, uyumsuzluk kaybı denilen bir elektrik kaybı olacaktır. Uyumsuzluk koşulları, cam kırılması, üretim sürecinin neden olduğu kusurlar ve kısmi gölgelenme gibi çevresel etkiler nedeniyle ortaya çıkar.

Genellikle uyumsuzluk meydana getiren parametreler açık devre voltajı ve kısa devre akımıdır. PV hücreleri seri bağlandığında kritik parametre kısa devre akımıdır. PV hücreleri paralel bağlandığında, kritik parametre açık devre voltajıdır. İmalat işleminden kaynaklanan uyumsuzluk kayıpları genellikle küçük kayıplardır ve imalat toleransları ile telafi edilir. Ancak, gölgelemenin neden olduğu uyumsuzluk kayıpları genellikle büyük kayıplardır.

Bir PV hücresi bulutların, ağaçların, binaların vs. gölgelenmesi nedeniyle güneş ışığı almadığında, buna kötü hücre denir. Dizideki bir hücre akım üretemez, yani kötü bir hücre haline gelirse, diğer hücreler tarafından ters gerilim bölgesinde çalışmaya zorlanır. Bu durum, kötü hücrenin diğer hücrelere yük olarak etki edeceği ve ısıyı dağıtmaya başlayacağı anlamına gelir. Bu durum p-n bağlantısının bozulmasına, lehimin PV modülünde erimesine ve kaplama malzemesine zarar vermesine neden olabilir. Bu durum, PV panelde sıcak nokta olarak adlandırılır. Sıcak nokta durumunu önlemek için, dizede baypas diyotları adı verilen ek diyotlar kullanılır. PV dizisindeki baypas diyotlarının kullanımın amacı, PV hücresindeki ters gerilimi sınırlamak ve delinme gerilimine ulaşmasını engellemektir.

Gölgelenme olmadığı durumlarda, PV sisteminin güç-gerilim karakteristiği yalnızca bir maksimum güç noktasına sahiptir. Ancak toz, ağaçlar, çevredeki yüksek binalar nedeniyle PV sistemlerde kısmi gölgeleme koşulları (PSC) meydana gelir. Bu durum oluştuğunda, PV sisteminin güç-gerilim eğrisinde, baypas diyotları nedeniyle birden fazla tepe noktası oluşur. Bu tepe noktalarına global maksimum güç noktası (GMPP) ve yerel maksimum güç noktaları (LMPP) denir. Bu durum, maksimum güç noktası takibi (MPPT) işlemini zor bir görev haline getirmektedir.

Fotovoltaik sistemlerin verimlilik ve yüksek yatırım maliyeti gibi bazı temel dezavantajları vardır. Bu durum nedeniyle, PV sistemlerinin maksimum verimlilikte çalıştırılması gerekir. Maksimum güç noktası izlemenin (MPPT) önemi bu noktada ortaya çıkmaktadır. Maksimum güç noktası takibi, MPPT dönüştürücüler tarafından yerine getirilen PV sistemden maksimum güç elde etme işlemidir. MPPT dönüştürücü terimi, MPPT algoritmasını, DC-DC çeviricinin kontrolcüsünü ve DC DC çeviriciyi içerir. Son yıllarda literatüre farklı MPPT yöntemleri sunulmuştur. Bunlar Parçacık Sürü Optimizasyonu, Gri Kurt Optimizasyonu, yapay zeka tabanlı yöntemler, Çiçek Tozlaşma Algoritması ve daha fazlasını içerir.

MPPT algoritmasının görevi, PV sisteminin maksimum güç noktasını bulmaktır. MPPT algoritmasının kontrol parametreleri çoğunlukla görev döngüsü ve voltajdır. Görev döngüsü kontrolü durumunda, MPPT algoritması güç çeviricisinin PWM sinyalini kontrol eder. Bununla birlikte, gerilim kontrolü durumunda MPPT algoritması, güç dönüştürücünün kontrolörüne bir referans voltajı verir. Güç çeviricisinin kontrolcüsü PI kontrolcüsü veya Bulanık mantık kontrolcüsü olabilir. Literatürdeki MPPT sistemi için en yaygın güç çeviriciler, alçaltan çevirici, yükselten çevirici, alçaltan yükselten çevirici ve SEPIC çeviricidir.

MPPT için kullanılan güç çevirici, çoğunlukla PV sisteminin çıkışına bağlanır ve bir PWM sinyali tarafından sürülür. Güç çeviricilerinin tasarımındaki ana parametreler endüktans ve kapasitanstır. indüktans, çeviricinin çalışma modunu etkiler. Endüktans çok küçük seçilirse, dönüştürücü çıkışı dengesiz hale getiren süreksiz akım modunda çalışacaktır. İndüktans çok büyük seçilmişse, çevirici yavaş bir geçici tepkiye sahip olacaktır. Kapasitans, gerilim dalgalanmalarını etkiler ve istenen dalgalanma yüzdesini korumak için hesaplanması gerekir. Kapasitans çok küçük seçilirse, dalgalanma gerilimi çok büyük olacaktır. Bu değer çok büyük seçilmişse, çevirici yavaş bir geçici tepkiye sahip olacaktır.

Bu tezin ana katkısı, kısmi gölgelenme koşullarında PV sistemin maksimum güç noktası takibi için kelebek optimizasyon algoritmasını uygulayarak maksimum güç noktasına ulaşma süresini azaltmaktır. Böylece, gerçek zamanlı uygulamalarda ihtiyaç duyulan takip hızı nedeniyle PV sistemlerinin değişken PSC altında performansını artırmak için literatüre önemli bir alternatif sunulmuştur. PV

dizin, yükselten çevirici, MPPT kontrolcüsü ve yükten oluşan sistem MATLAB/Simulink ile modellenmiş olup BOA, PV dizisindeki üç farklı gölgelenme senaryosu için uygulanmıştır. BOA'nın sonuçları, PSO-GSA ve GWO algoritmalarıyla karşılaştırmalı bir analizle doğrulanmıştır. Sonuçlar, BOA'nın son literatürdeki bu algoritmalardan daha yüksek doğruluk ve daha iyi takip hızı verebileceğini göstermektedir.

ACKNOWLEDGEMENTS

I would like to express my heartfelt thanks to Prof. Dr. Mehmet TÜMAY for his supervision, guidance, encouragements, and continuous confidence in me throughout this thesis. It has been a great honor to have Prof. Dr. Mehmet TÜMAY as a supervisor.

I am also grateful to Asst.Prof.Dr. Tuğçe DEMİRDELEN not only for her guidance and encouragements as a co-supervisor but also for her unforgettable and valuable contributions to my career.

I would like to thank Assoc. Prof. Dr. Mehmet Uğraş CUMA, Asst.Prof.Dr. Adnan TAN and Asst.Prof.Dr. Murat Mustafa SAVRUN for accepting to be a member of the examining committee for my thesis.

I also thank Asst.Prof.Dr. Fırat EKİNCİ, Res. Asst. Burak ESENBOĞA, Res. Asst. Abdurrahman YAVUZDEĞER and Res. Asst. Murat ÇIKAN for their valuable discussions and technical help.

My appreciation is also extended to my colleague Res. Asst. Halit ERİŞ from Çukurova University for his valuable advice and supports.

Finally, I would like to express my deepest gratitude to my family, for their patience, encouragement and continuous support.

CONTENTS **PAGE**

LIST OF TABLES **PAGE**

LIST OF FIGURES **PAGE**

LIST OF SYMBOLS

I_d	:	PV Cell diode current
I_0	:	PV cell reverse saturation current
k	:	Boltzmann constant
a	:	Diode ideality constant
q	:	Electron charge
I_{pv}	:	PV current generated by sunlight
K_I	:	Short circuit temperature coefficient
S	:	Solar irradiance
E_{GO}	:	Bandgap energy of silicon
T_r	:	Reference temperature
I_{SC}	:	Short circuit current
I_{or}	:	Saturation current
V_{in}	:	Input voltage
V_0	:	Output voltage
D	:	Duty cycle
I_L	:	Inductor current
I_{in}	:	Input current
$I_{L,min}$	:	Minimum ripple current
$I_{L,mac}$	:	Maximum ripple current
$L_{critical}$	:	Critical inductance
C	:	Capacitance
R	:	Resistance
f	:	frequency
T	:	Temperature (K)
R_{eq}	:	Equivalent resistance seen from PV side
R_{in}	:	Equivalent resistance of PV source

V_i^{k+1}	:	Velocity of ith particle at (k+1)th iteration
c	:	Weights
P_{best}	:	Best position of a particle
g_{best}	:	Best position of all particles
G	:	Gravitational constant
M_1, M_2	:	Masses of particles
a	:	Acceleration
F	:	Force
M	:	Mass
q_i	:	Strength of mass i
f_i	:	Fitness function
X_p	:	Position vector of the prey
f_i	:	Fragrance of the ith butterfly
x_t^i	:	Solution vector
g^*	:	The best solution in current iteration

LIST OF ABBREVIATIONS

ANFIS	:	Adaptive neuro-fuzzy inference system
ANN	:	Artificial Neural Network
BOA	:	Butterfly Optimization Algorithm
CDV	:	Cross diagonal view
CIAFSA	:	Comprehensive improvement on the AFSA
DLCI	:	Dynamic leader based collective intelligence algorithm
FOCV	:	Fractional Open Circuit Voltage
GA	:	Genetic Algorithm
GMPP	:	Global maximum power point
GSA	:	Gravitational Search Algorithm
GSS	:	Golden section search
GWO	:	Grey Wolf Optimization Algorithm
HIL	:	Hardware in loop
IC	:	Incremental Conductance
LMPP	:	Local maximum power points
MAE	:	Mean Absolute Error
Modified AFSA	:	Modified artificial fish swarm algorithm
MPPT	:	Maximum Power Point Tracking
MSSA	:	Memetic Salp Swarm Algorithm
P&O	:	Perturb and Observe
PSC	:	Partial Shading Condition
PSO	:	Particle swarm optimization
PV	:	Photovoltaic
P-V	:	Power-Voltage
RE	:	Average Relative Error
RMSE	:	Root Mean Square Error
SEPIC	:	Single-ended primary-inductor converter
STD	:	Standard Deviation

1. INTRODUCTION

1.1. Overview

Increasing energy demand during the last decade and the depletion of fossil fuels have led governments and energy companies to look an alternative energy source that is sustainable. Among the alternatives, solar energy is the most promising one because of its availability all around the world. There are different ways to use solar energy as electricity. The prominent way is to use Photovoltaic (PV) Cells to convert solar energy into electricity. Photovoltaic systems are preferred due to their advantages like sustainability, environment-friendly nature. The main disadvantage of PV systems is their high investment costs. This condition requires the system to operate efficiently. The main concept that affects the efficient operation of PV systems is the maximum power point. The operation of keeping the PV system at its maximum power point is called the maximum power point tracking (MPPT).

MPPT is a process usually implemented with a power converter in order to increase the performance of a PV system. The operation point of PV system changes nonlinearly with the change in environmental parameters such as temperature and solar irradiation. MPPT ensures the operation of the PV system at its maximum point regardless of the changes in the temperature and solar irradiation. MPPT has been carried out by using various algorithms. It has been a popular topic in recent literature to find an MPPT algorithm and a circuit configuration for PV systems that operate properly under variable environmental conditions.

MPPT under non-uniform insolation is a more difficult task and different approaches have been proposed for this purpose in the recent literature. The non-uniform insolation on the PV system is also known as partial shading condition (PSC).

Partial shading conditions occur because of shadows of objects such as clouds, long buildings, trees, etc. The reason for this complexity of MPPT under partial shading conditions is the occurrence of local peaks on the power-voltage (P-V) curve of the PV system. The conventional MPPT algorithms are able to converge the maximum power point (MPP) under uniform insolation. But under PSC they could not track the MPP. In the recent literature soft computing techniques such as fuzzy logic control, artificial neural networks (ANN) and bio-inspired algorithms have been implemented for complicated optimization problems. Since the MPPT under PSC is an optimization problem, these techniques have been implemented for the MPPT under PSC. The soft computing techniques used for the MPPT under PSC is shown in Figure 1.1.

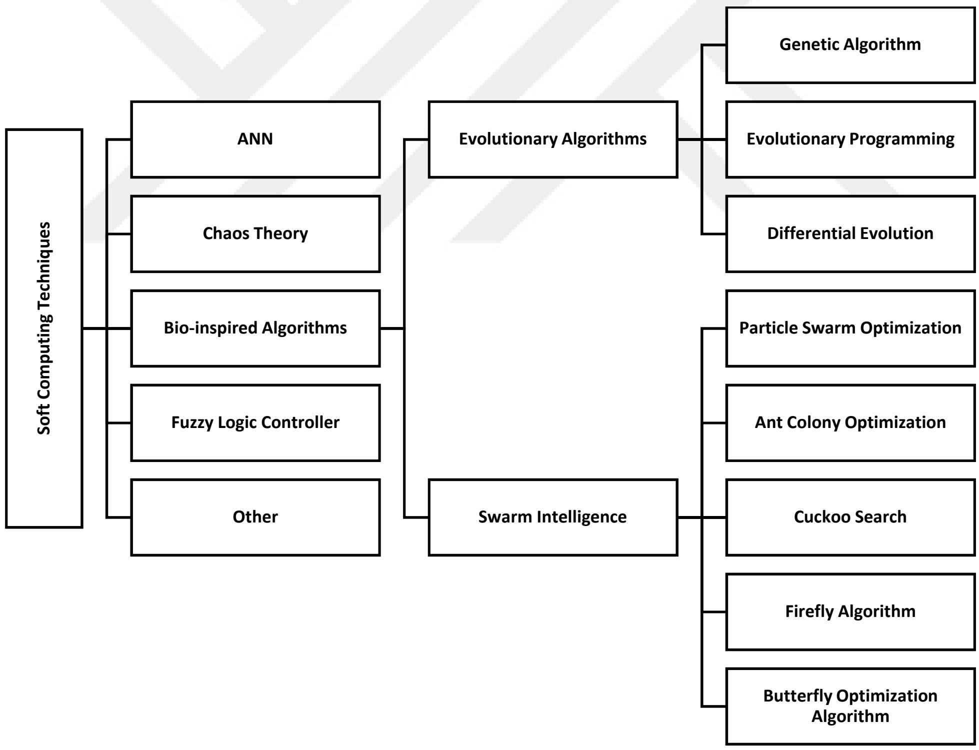

Figure 1.1 Soft computing techniques implemented for the MPPT under PSC (Li et al., 2018a)

1.2. Objective and Outline of the Thesis

The main objective of this thesis is to implement a new MPPT algorithm for a PV system to increase its efficiency under PSC. For this purpose modeling and simulation of a PV system that consists of a PV array, DC-DC Boost converter, and DC load is carried out by using MATLAB/SIMULINK. A new soft computing MPPT algorithm and two other algorithms from the recent literature is implemented for the MPPT under PSC on this modeled system.

After the introduction section where an overview and objective of the thesis is given the outline of the thesis is as follows;

Chapter 2 gives a comprehensive literature survey about PV systems and MPPT techniques that are implemented on the PV systems under PSC.

In Chapter 3 types of PV cells, mathematical modeling of PV systems, the effect of temperature and solar irradiation on PV cells, PV module and PV array concepts, mismatch losses on PV arrays, characteristics of PV systems under PSC are presented.

In Chapter 4 the term maximum power point tracking converter that comprises MPPT algorithms, MPPT controller and DC-DC converters are presented in detail

In Chapter 5, the simulation results of the PSO-GSA, GWO and BOA algorithms are presented in detail and performance comparison is made.

2. LITERATURE SUMMARY

The Flower Pollination Algorithm for MPPT of a building-integrated PV system to mitigate the effects of partial shading is proposed (Diab and Rezk, 2017). PSO and Differential Evolution algorithms are used as references to test the proposed algorithm. It is stated that the proposed algorithm has better performance than the other two algorithms. The implementation of PSO algorithm to MPPT of PV systems under PSC is presented (Dileep and Singh 2017). The authors validated the proposed algorithm on a 110 W PV system. The cross diagonal view (CDV) configuration to mitigate the effect of PSC on the PV system is proposed (Bosco and Mabel, 2017). The authors stated that in the proposed configuration, the physical position of PV modules is changed without changing their electrical connections. Hence the shading on the PV system is distributed. The effect of the proposed configuration is compared with conventional configurations and it is seen that the proposed configuration provides %21.67 more power than other configurations.

A GMPPT algorithm based on power increment is presented and analyzed by both simulation and experiments (Li et al., 2018b). It is seen that the proposed algorithm has the best convergence speed under different shading patterns.GWO and FLC are implemented to MPPT of PV systems under PSC against the problems like failure of tracking GMPP in case of position change of GMPP and oscillation around GMPP increased when the other algorithms such as PSO and CSO are implemented (Eltamaly and Farh, 2019). Dynamic leader based collective intelligence algorithm (DLCI) is implemented to MPPT of PV system under PSC (Yang et al., 2019a). A comparative study is conducted between the proposed algorithm and algorithms available in the literature such as Incremental Conductance (IC), genetic algorithm (GA) CSO and whale optimization algorithm. The algorithms are implemented both on Hardware-in-the-loop (HIL) test and 4 different case studies. It is seen that the proposed algorithm is able to increase PV system power up to 36.64% and decreases the fluctuations on the power up to 21.17%.

An algorithm is proposed for MPPT under PSC (Murtaza, Chiaberge, et al. 2014). The authors validated the algorithm by using the real data of 86.2 kW building on MATLAB/Simulink. Modified differential evolution algorithm is implemented for the MPPT under PSC (Ramli et al., 2015). The algorithm is validated by comparing its results with the PSO algorithm. It is seen that while the proposed algorithm converges GMPP, PSO converges LMPP. An MPPT method for PSC based on artificial vision is proposed (Martin et al., 2018). A webcam is used to specify the shading pattern on the PV panel. The reference signal generated according to the shading on the PV panel is used to track the GMPP. It is seen that the efficiency of the proposed method is between 98.1% and 99.6%.

Memetic Salp Swarm Algorithm (MSSA) is applied to the GMPPT of PV systems (Yang et al., 2019b). The algorithm is validated by MATLAB/Simulink and HIL experiment. It is seen that compared to GWO, GA, and PSO, the results of the proposed algorithm has fewer power fluctuations under the step change of solar radiation.PSO and Perturb and Observe (P&O) combined for tracking the MPP under PSC (Sundareswaran et al., 2015). The hybrid algorithm is tested both by simulation and experiments. When the proposed algorithm is compared with the PSO algorithm. It is seen that the fluctuations on the current and voltage graphs at the output of the converter is lesser when the proposed algorithm is used.4 MPPT methods are implemented for the GMPPT under PSC (Mohamed et al., 2019). The algorithms are validated on MATLAB/Simulink by comparing the PSO algorithm. PSO and variable step P&O algorithms are combined for the GMPPT of the PV system (Mao et al., 2019). The proposed method is compared with PSO and classic P&O methods by simulations. It is seen that the proposed method has fewer oscillations on the output than the other two algorithms.

An Adaptive neuro-fuzzy inference system (ANFIS) based GMPPT method is presented (Belhachat and Larbes, 2017). The authors tested the proposed method under different shading patterns and changing solar radiance. It is seen that the algorithm can track GMPP with high efficiency and high speed. A Simulated Annealing (SA) based GMPPT method is presented (Lyden and Haque, 2016). The algorithm is tested by both simulations and experimental analysis. Authors analyzed its performance by comparing PSO and P&O algorithms. Fireworks Algorithm (FWA) and P&O are combined to track GMPP of PV systems under PSC (Manickam et al., 2017). Under uniform insolation P&O and in the presence of a shading condition FWA is used to track GMPP of the system. The proposed method is validated by experiments. Modified artificial fish swarm algorithm (Modified AFSA) is applied to the MPPT of PV panels under PSC (Mao et al., 2016). The proposed algorithm and PSO are compared with simulation analysis by using MATLAB/Simulink. It is seen that the proposed method has better performance results than the PSO algorithm. Fractional Open Circuit Voltage (FOCV) and IC methods are combined to track MPP of PV systems under PSC (Javed et al., 2016). In the proposed method, FOCV determines the boundaries for the GMPP after that IC is used to converge the GMPP. The algorithm is validated by simulations by using MATLAB/Simulink.

Conventional MPPT methods like P&O and IC are combined with Artificial Neural Network (ANN) for GMPPT of PV system (El-Helw et al., 2017). In the proposed method ANN describes the boundaries of GMPP and after that, the conventional algorithm converges to the GMPP. The proposed hybrid method and the ANN is compared by simulations. It is concluded that the proposed method is faster than the ANN while tracking the GMPP. Improved Differential Evolution algorithm based GMPPT method is presented (Tey et al., 2018). The proposed method is analyzed by simulations using PSIM. It is seen that the algorithm is able to converge GMPP with %99 accuracy, 2s oscillation time and 0.1s response time to the load variations. An improved P&O is presented for the GMPPT under PSC

(Kapić et al., 2018). It is stated that the proposed method is also appropriate for the variable solar radiance conditions.

A novel GMPPT algorithm for the PSC is presented (Baimel et al., 2018). In the proposed method, the Power-Voltage curve of the PV system divided into regions. At first, the region of the GMPP is determined. After that classic P&O algorithm is used to converge GMPP in the chosen region. The proposed method and P&O, Ant Colony Optimization based MPPT algorithms are tested by simulations with different shading conditions. It is seen that the proposed algorithm showed better performance than the other two algorithms. A method for detecting the presence of shading condition and the number of shaded cells is presented (Davies et al., 2018). The proposed method uses the occurrence of “knee voltage” in the Current-Voltage curve of the PV system. The proposed method is validated experimentally.

A Dual Port Step-up Gain Converter is presented for PV application on the rooftop of a train (Raizada and Verma, 2018). Thanks to the fast response feature of the proposed converter it can be implemented for the moving PSC. A combined ANN-P&O method is implemented for the GMPPT of the PV system under PSC (Oubbati et al., 2018). The region of the GMPP is determined by ANN and after that P&O algorithm is used to converge the GMPP inside this region. The presented method is validated by the simulation analysis and it is seen that it is able to track GMPP effectively. AFSA is optimized by using PSO algorithm (Mao et al., 2018). The proposed algorithm is called comprehensive improvement on the AFSA (CIAFSA). It is validated by simulations using MATLAB-Simulink.

Golden section search (GSS) based GMPPT algorithm is presented (Malathy and Ramaprabha, 2018). The proposed algorithm tracks the GMPP with two steps. In the first step, the search is restricted near to the GMPP. In the second step, the algorithm converges the GMPP in this region. The presented algorithm is validated under different shading patterns and it is stated that the proposed method is effective to track GMPP under PSC.FP algorithm is proposed for GMPPT under

PSC (Shang et al., 2018). The proposed method is compared with PSO and P&O and it is stated that the proposed method can efficiently track GMPP under PSC. An adaptive fuzzy logic based MPPT is proposed (Choudhury and Rout, 2015). It is stated that the proposed algorithm has better tracking performance than conventional algorithms.

Table 2.1. The summary metaheuristic algorithms implemented for MPPT of PV panels under PSC

Ref.	**MPPT Algorithm**	**Control Parameter**	**Converter Type**	**Contribution**
(Diab and Rezk, 2017)	Flower Pollination Algorithm	Duty Cycle	Boost Converter	Proposed the Flower Pollination Algorithm
(Li et al., 2018b)	Power Increment Based GMPPT Algorithm	Duty Cycle	Buck-Boost Converter	Proposed Power Increment Based GMPP Algorithm
(Yang et al., 2019a)	DLCI	Duty Cycle	Buck-Boost Converter	Proposed DLCI for GMPPT
(Martin et al., 2018)	MPPT based on Artificial Vision	Duty Cycle	Buck-Boost Converter	Proposed MPPT algorithm based on Artificial Vision
(Yang et al., 2019b)	MSSA	Duty Cycle	Boost Converter	Proposed MSSA based MPPT algorithm
(Belhachat and Larbes, 2017)	ANFIS	Duty Cycle	Buck-Boost Converter	Proposed MPPT method based on ANFIS
(Lyden and Haque, 2016)	SA	Voltage	Boost Converter	Proposed MPPT method based on SA
(Tey et al., 2018)	Improved Differential Evolution	Duty Cycle	SEPIC Converter	Proposed Improved Differential Evolution based GMPPT algorithm
(Baimel et al., 2018)	Segmentation Algorithm	Duty Cycle	Boost Converter	Proposed Segmentation Algorithm
(Mao et al., 2018)	CIAFSA	Voltage	Boost Converter	Improved the performance of AFSA
(Malathy and Ramaprabha, 2018)	GSS	Duty Cycle	Boost Converter	Proposed GSS based two-stage GMPPT algorithm

3. PHOTOVOLTAIC SYSTEMS

Humans have tried to use solar energy in different ways. At first, there were some primitive attempts, for example, Greeks used solar energy to heat their houses in the 5th century BC. In USA solar energy is used to heat water. In Europe, a solar-powered steam engine is invented in the late 19th century. These are called passive solar systems. In the second quarter of the 19th century, a phenomenon called the photovoltaic effect is discovered by Edmund Becquerel. Becquerel was studied with selenium and his system had an efficiency of about 2%. After the first half of the 20th century, silicon Photovoltaic (PV) cells are developed in the Bell Labs by scientists. It had an efficiency of 4% but after some development increased up to %11. These cells were able to convert the solar irradiance into electricity. At first, they are implemented for applications such as satellites. However, after the development of its technology the prices were reduced. So, PV cells started to be implemented for regular applications.

Nowadays as the development of the industry increases, the need for electrical energy also increases. Due to the depletion of fossil fuels and their negative environmental impacts, scientists have focused on the development of renewable energy technologies. Among renewable energy sources, solar energy is the most promising type due to the fact that it is easily accessible all over the world. Solar energy is converted to the electricity by using PV cells. The characteristics of these cells depend on some environmental parameters such as ambient temperature and solar irradiance.

3.1. PV Cell

By using the PV technology of today, only 18-20% of the available solar energy is converted to electrical energy. According to this data, it can be said that converting the solar energy to electrical energy is inefficient. The main limiting factor here is the nature of the sunlight and the semiconductor material used in the PV cell. The sunlight comprises the shortest and the longest wavelengths of electromagnetic radiation at the same time. The shortest wavelengths are called ultraviolet, while the longest wavelengths are called infrared. The wavelengths between these two are called the visible light. Among these, ultraviolet has highest energy, silicon (Si) which is the most common PV cell material cannot absorb shorter wavelengths as good as other semiconductor materials such as gallium arsenide (GaAs) and germanium (Ge). When the sunlight is absorbed by the PV cell, photons of the sunlight generate electron-hole pair in the semiconductor material. Figure 3.1 shows the generation of electron-hole pair in the silicon PV cell.

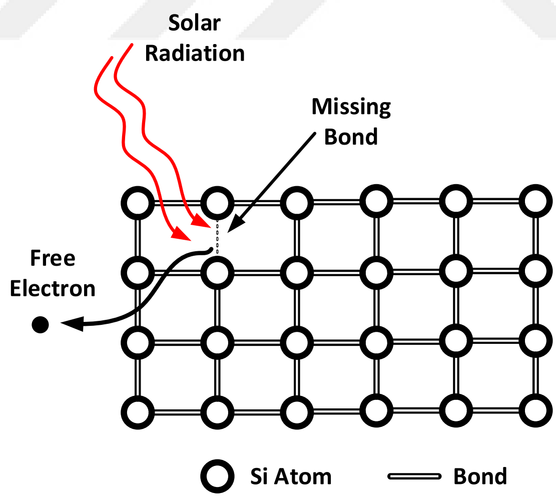

Figure 3.1. The generation of electron-hole pair in the Silicon PV Cell

3.1.2. Types of PV Cells

The PV cells are categorized into 5 different types as shown in Figure 3.2.

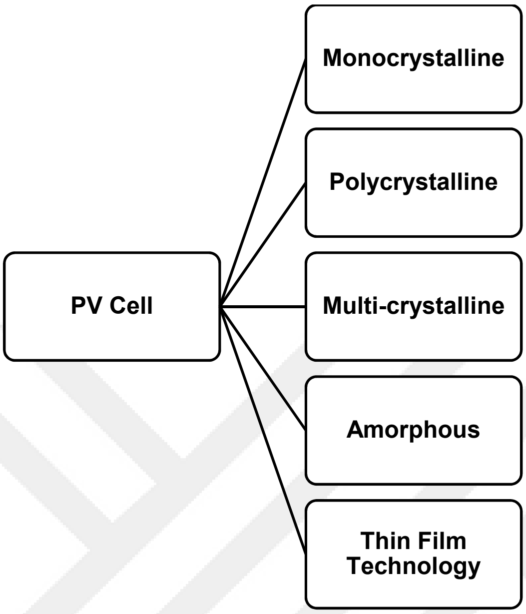

Figure 3.2. Types of the Silicon PV Cell

Among the types of Silicon PV cells, Monocrystalline cells have the highest efficiency rate (18 to 20%). However, this type has the highest manufacturing cost. Multi-crystalline and polycrystalline cells have more economic manufacturing process and less efficiency (16 to 18%). Amorphous silicon cells have the cheapest manufacturing process and the lesser efficiency (8 to 10%). Thin film technology is the deposition of layers of amorphous silicon cells on a stainless-steel ribbon. The efficiency of thin-film technology is 5 to 13%. The average service life of the monocrystalline PV cells is 25 to 30 years, for the polycrystalline, it is 20 to 25 years, for thin-film technology it is 15 to 20 years.

Scientists developed a new technology called proton enhanced thermionic emission (PETE) that increases the efficiency of the PV system up to 50% (Kribus and Segev, 2016). In this process, both heat and light are used to generate electricity. For the traditional PV technology, efficiency decreases with the increasing temperature. However, for PETE a thermal converter is used for capturing the waste heat. Hence, the increasing temperature increases the efficiency.

One of the methods aimed to increase the PV system efficiency suggests stacking PV cells of different semiconductors. By doing so, each semiconductor material absorbs a different part of the spectrum. Hence the absorption range of wavelength of the sunlight is increased. This method has increased the efficiency of up to 40%.

3.1.3. Modelling of PV Cell

The ideal equivalent circuit of the PV cell is shown in Figure 3.3. The equation for the current I is given by Equation 3.1.

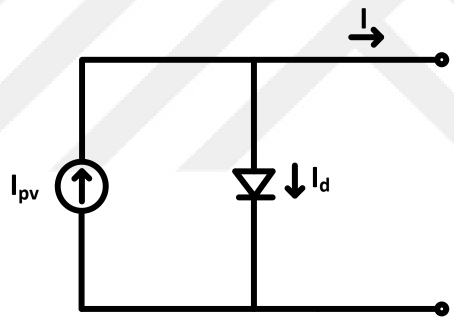

Figure 3.3. The ideal model of PV cell

$$I = I_{pv} - I_d \quad (3.1)$$

I_d in Equation 3.1 is described in Equation 3.2.

$$I_d = I_0[\exp\left(\frac{qV}{akT}\right) - 1] \quad (3.2)$$

Where I_{PV} is the PV cell current generated by the phenomenon shown in Figure 3.1. I_d is the diode current, I_0 is the reverse saturation current, k is the

Boltzmann constant, T is the temperature of the diode, a is the diode ideality constant and q is the electron charge

For practical PV applications, in order to get the desired voltage and current values, parallel and series combinations of PV cells are created. The practical equivalent circuit of PV cell is shown in Figure 3.4.

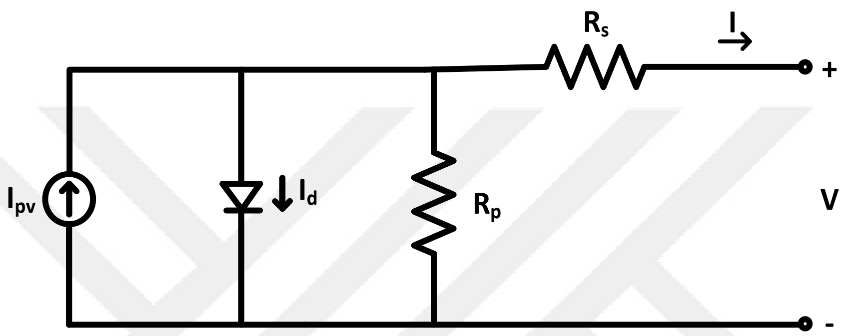

Figure 3.4.The practical model of PV cell

The current I in Figure 3.4. is expressed in Equation 3.3.

$$I = I_{pv} - I_0 \left[\exp\left(\frac{V+R_s I}{V_t a}\right) - 1\right] - \left(\frac{V+R_s I}{R_p}\right) \quad (3.3)$$

I_o and I_{pv} in Equation 3.3 are expressed in Equations 3.4 and 3.5 respectively.

$$I_0 = I_{or} \exp\left[\frac{qE_{GO}}{bk\left(\left(\frac{1}{T_r}\right)-\left(\frac{1}{T}\right)\right)}\right]\left(\frac{T}{T_r}\right)^3 \quad (3.4)$$

$$I_{pv} = \frac{S[I_{sc}+K_I(T-25)]}{1000} \quad (3.5)$$

In Equations 3.4 and 3.5; I_0 is leakage current, I_{pv} is PV current generated by sunlight, a and b stands for the ideality factor, K_I stands for the short circuit temperature coefficient, S stands for the solar irradiance (W/m^2), E_{GO} stands for the bandgap energy of silicon, T_r stands for the reference temperature, I_{sc} stand for the short circuit current, I_{or} stands for the saturation current.

When a manufacturer produces a PV panel, they provide important electrical characteristic parameters belong to this panel rather than its mathematical equations. These parameters are shown in Figure 3.5.

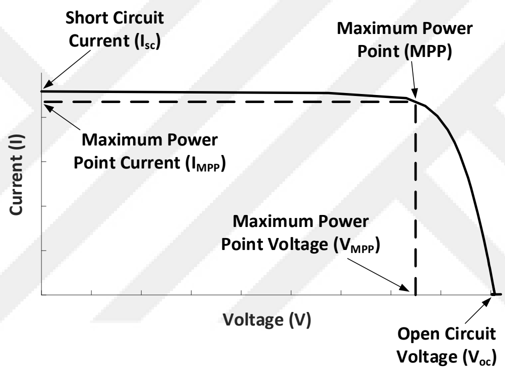

Figure 3.5.The Current-Voltage Characteristic Curve of PV Cell

Short circuit current is the current value measured when the terminals of the PV cell is short-circuited, Open circuit voltage is the voltage value measured when there is no load connected to the terminals of the PV cell. V_{MPP} and I_{MPP} are voltage and current values of the PV cell at the maximum power point.

3.2. The Effect of Solar Irradiance and Temperature on PV Cells

The power output of a PV module is directly depending on the panel temperature and the solar irradiance as described in Equation 3.5. Figure 3.6 and Figure 3.7 shows the effect of solar irradiance and temperature on the I-V and P-V characteristics of the PV panel.

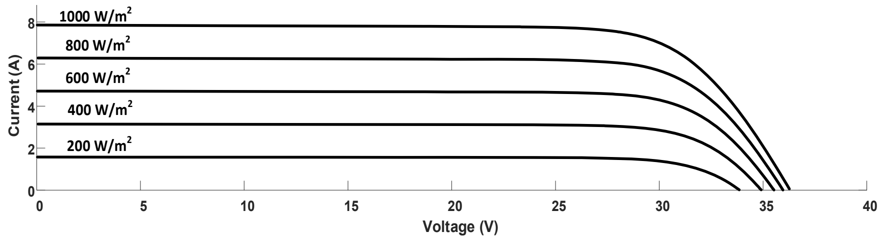

Figure 3.6. The effect of solar irradiance on the I-V curve

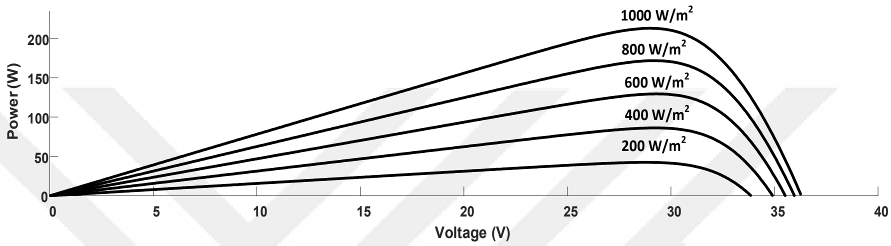

Figure 3.7. The effect of solar irradiance on the P-V curve

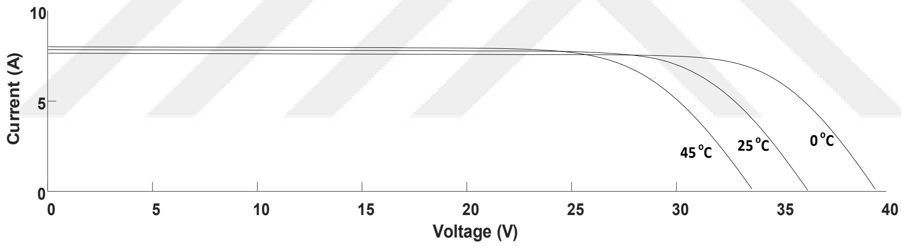

Figure 3.8. The effect of temperature on the I-V curve

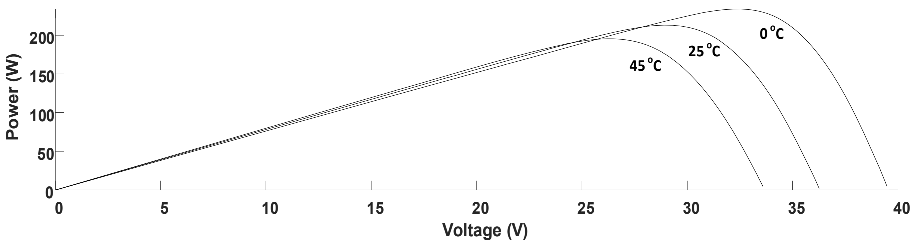

Figure 3.9. The effect of temperature on the P-V curve

From Figure 3.6 and Figure 3.7, it is seen that as the solar irradiance on the PV module increases the current at the same voltage increases. Hence the maximum power point of the module increases.

Figure 3.8 and Figure 3.9 show the effect of the change of the temperature while the solar irradiance is constant. It is observed that as the temperature increases, the maximum voltage decreases. Hence the maximum power point of the module decreases.

3.3. PV Module and PV Array

Current and Voltage ratings of a PV cell is not appropriate to use it alone for most of the applications. The typical open-circuit voltage of a PV cell is around 0.6 V that is much lower than the rated voltage of most electrical systems. To increase the voltage level, many PV cells is connected series. For example, PV modules with 36 series-connected PV cells are manufactured for 12 V battery applications. The module has open circuit voltage around 21 V and maximum power point voltage around 17 V that is suitable for charging 12 V batteries under ordinary insolation conditions. Similar to the series connection, PV cells are connected parallel to increase the rated current of a module. As the power rating of the application increases such as grid-connected applications, the number of series and parallel connected cells in a module also increases. Figure 3.10 and Figure 3.11 show the Current-Voltage characteristic graphs of a single PV cell and two PV cells connected in series and parallel respectively.

Just like PV cells, the same parameters are valid for PV modules. PV modules are connected in series and parallel combinations to increase the current and voltage ratings. Figure 3.12 shows the illustration of the PV cell, PV Module and PV Array.

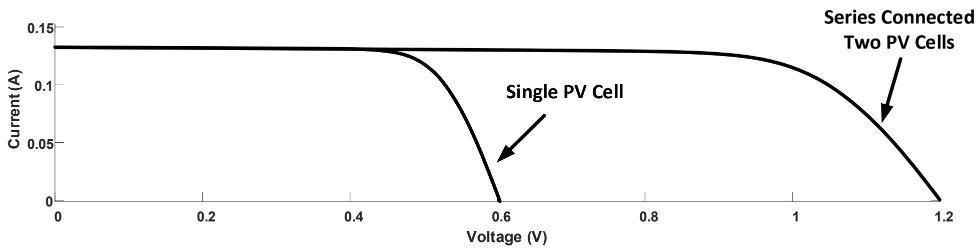

Figure 3.10. Current-Voltage Characteristics of PV Cells Connected in Series

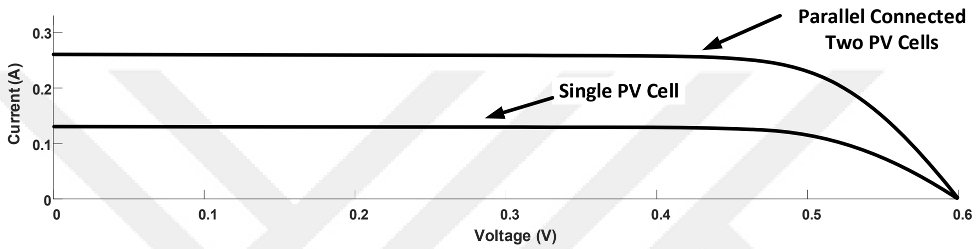

Figure 3.11. Current-Voltage Characteristics of PV Cells Connected in Parallel

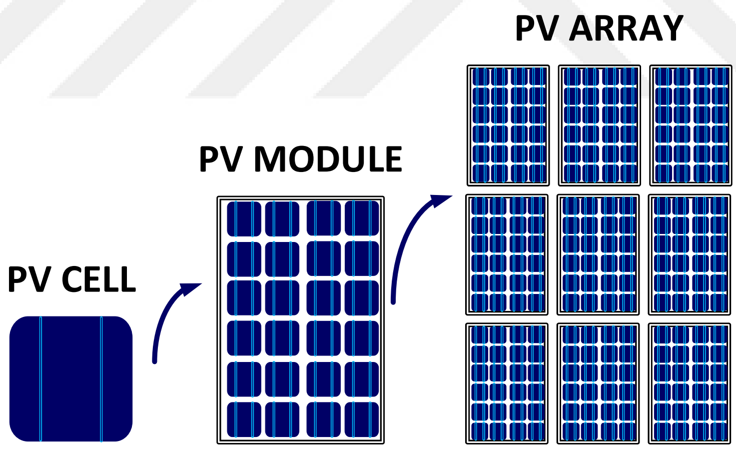

Figure 3.12. PV Cell, PV Module and PV Array

3.4. Mismatch Losses

During the manufacturing process, the PV cells are connected series and parallel based on the assumption that all cells have identical characteristics. But in practice when some of the parameters of one or more of the cells in the string differ from others, there will be an electrical loss called mismatch loss. Mismatch conditions occur due to the following reasons:

- The broken glass cover of the PV module,
- The parameter difference caused by the manufacturing process,
- Environmental effects such as partial shading.

Usually, mismatched parameters are open-circuit voltage (V_{oc}) and short circuit current (I_{sc}). When PV cells are connected in series the crucial parameter is I_{sc} and when PV cells are connected in parallel the crucial parameter is $V_{oc.}$ Mismatch losses caused by manufacturing process are usually small losses and compensated by manufacturing tolerances. But mismatch losses caused by shading are usually major losses. Figure 3.13 illustrates the mismatch condition of a PV cell in a PV string.

When a PV cell does not receive sunlight due to shading of clouds, trees, buildings, etc. it is called a bad cell. If one cell in the string unable to generate current i.e. become a bad cell, it will be forced to operate in the reverse bias region by other cells. This means the bad cell will act as a load to other cells and start to dissipate heat. This condition may cause the breakdown of the p-n junction, melting of the solder in the PV module and harm to the covering material. This condition is called the hot spot on the PV module.

Figure 3.13-a shows one bad cell in a PV string, while active cells generating power the bad cell is not able to supply the same current, therefore it is forced to operate in the reverse bias region. As the bad cell operates in the reverse bias region, it is subjected to the full power output of the active cells. This leads to the generation of the hot spot. Figure 3.13-b shows the equivalent circuit of the PV string that has a bad cell. The elements on the current path are green colored. The equivalent circuit of an active cell is shown in Figure 3.3. Due to the fact that the

current source of the bad cell is inactive, the current flows through its diode but in the reverse direction.

In order to prevent the hot spot condition, additional diodes called bypass diodes are used in the string. The use of bypass diodes is shown in Figure 3.13-c. In this figure, the elements on the current path are colored green, the bad cell is colored red and inactive cells are colored blue.

For maximum performance, a by-pass diode for each cell can be added to the circuit. But in order to decrease the cost, a by-pass diode is connected parallel to a group of cell. The drawback of this application is that the presence of the bad cell makes a few more active cells inactive. In Figure 3.13-c, it is seen that 2 more blue colored cells became inactive due to the presence of a bad cell.

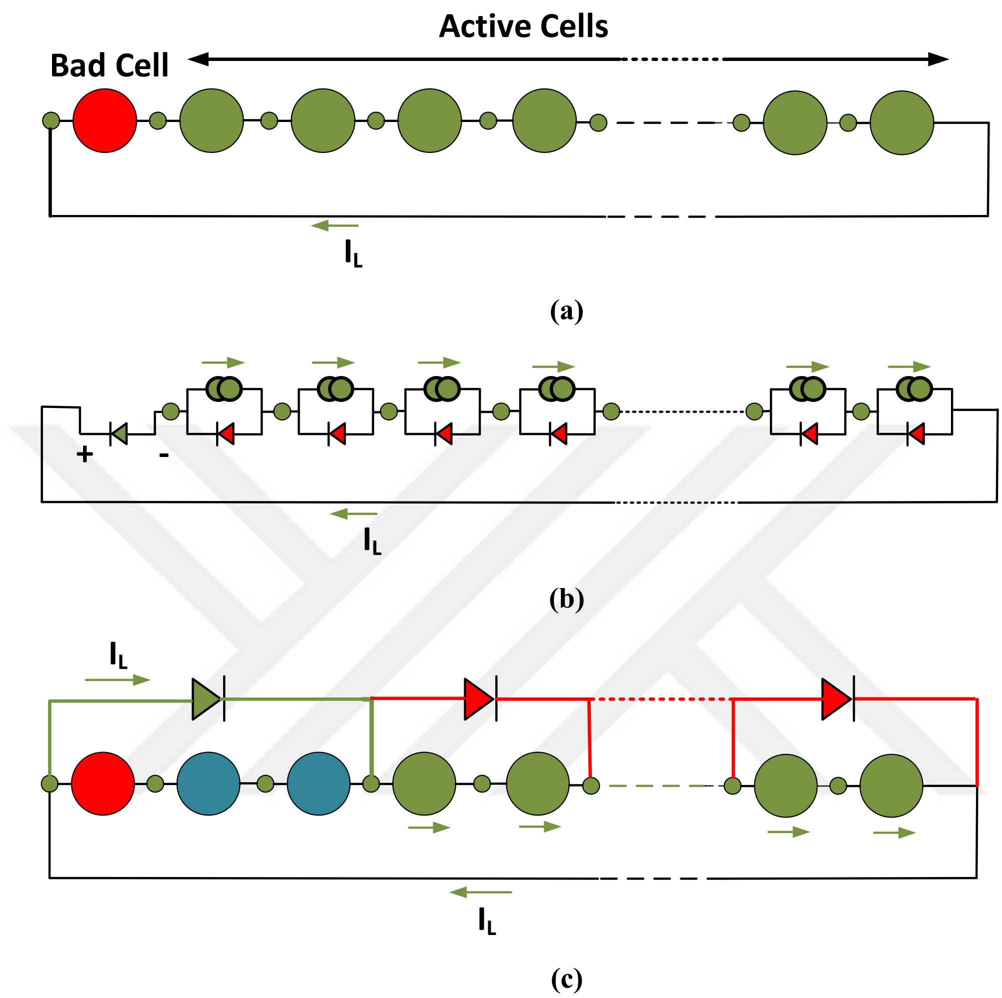

Figure 3.13. (a) A PV cell string with one bad cell (b) equivalent circuit of this string (c) PV cell string with by-pass diodes

Figure 3.14 shows the I-V characteristic curve of active and bad cells. It is seen from the figure that, the operation point of the bad cell is at the left side of the curve ie. reverse bias region. The purpose of using bypass diodes in the PV string is to restrict the reverse bias voltage on the PV cell and prevent it to reach the breakdown voltage.

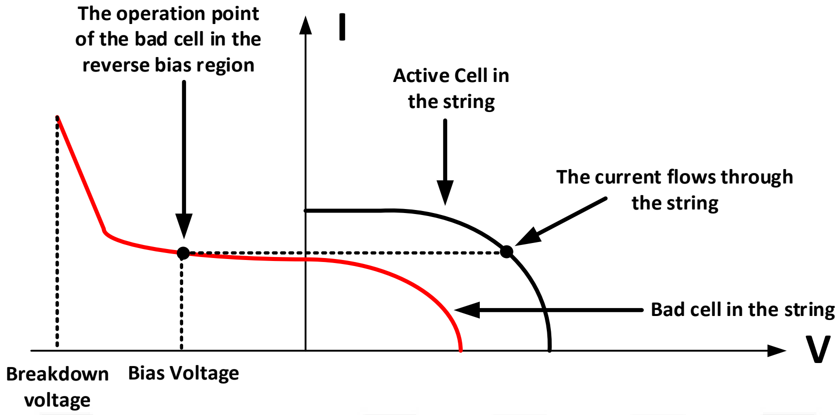

Figure 3.14. I-V Curve of Active and Bad Cell (Bidram et al., 2012)

3.5. PV Characteristics Under Partial Shading Conditions

Figure 3.15-a shows PV array under uniform insolation and Figure 3.15-b shows PV array under partial shading condition. The corresponding P-V and I-V curves of these PV arrays are shown in Figure 3.16. As seen from Figure 3.16, the uniform insolation (i.e. unshaded array) results in a characteristic that has one maximum powerpoint. But the different insolation level of panels on a PV array (i.e. partial shading) results in a characteristic that has multiple peaks because of bypass diodes.

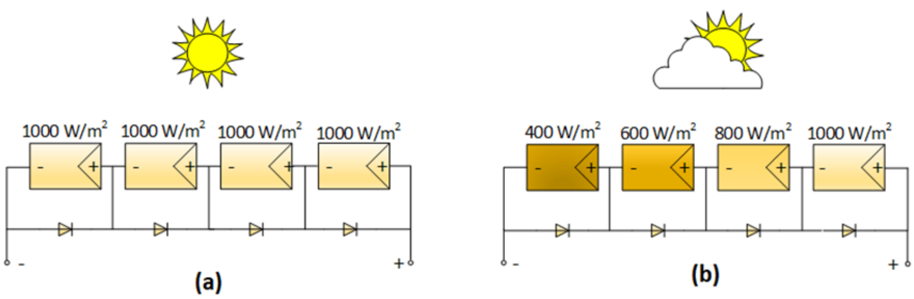

Figure 3.15. (a) PV array under uniform insolation (b) PV array under Partial Shading

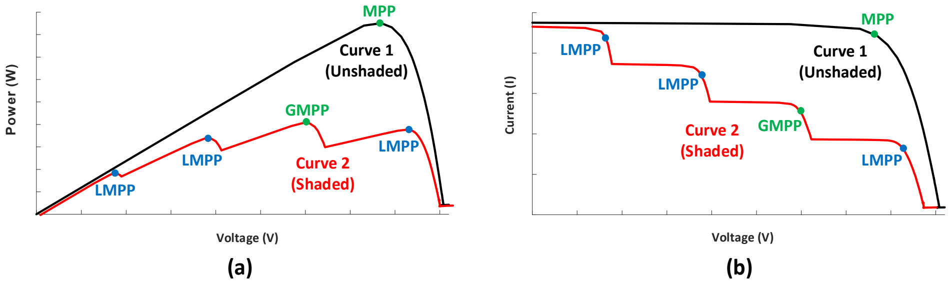

Figure 3.16. The Power-Voltage and Current-Voltage curves of the panels in Figure 3.15

4. MPPT CONVERTERS

Maximum power point tracking (MPPT) is a process of obtaining the maximum power from the PV module fulfilled by MPPT converters. The term MPPT converter comprises the MPPT algorithm, the controller of the power converter and the power converter. Different types of MPPT methods have been proposed to the literature during recent years. (Li et al., 2018a; Mohapatra et al., 2017; Sameeullah and Swarup, 2016; Seyedmahmoudian et al., 2016) This includes Particle Swarm Optimization, Grey Wolf Optimization, ANN-based methods, Flower Pollination Algorithm and more. The task of the MPPT algorithm is to find the maximum power point of the PV system. The control parameters of the MPPT algorithm are mostly duty cycle and voltage. In the case of the duty cycle, the MPPT algorithm controls the PWM signal of the power converter. However, in the voltage case, the MPPT algorithm gives a reference voltage to the controller of the power converter. The controller of the power converter may be a PI controller or the Fuzzy logic controller. The most common power converters for the MPPT system in the literature are a boost converter, buck converter, buck-boost converter, and SEPIC converter.

The power converter used for the MPPT mostly connected to the output of the PV system and driven by a PWM signal. The main parameters in the design of the power converters are inductance and capacitance. The inductance affects the operation mode of the converter. If the inductance is chosen too small then the converter will operate in the discontinuous current mode that makes the output unstable. If the inductance is chosen too large, then the converter will have a slow transient response. The capacitance affects the voltage ripples and needs to be calculated in order to maintain the desired ripple percentage. If the capacitance is chosen too small then the ripple voltage will be too large. If the capacitor is chosen too large then the converter will have a slow transient response.

4.1. DC-DC Converters

There are different types of DC-DC converters implemented for the MPPT of PV systems. The most common types are shown in Figure 4.1.

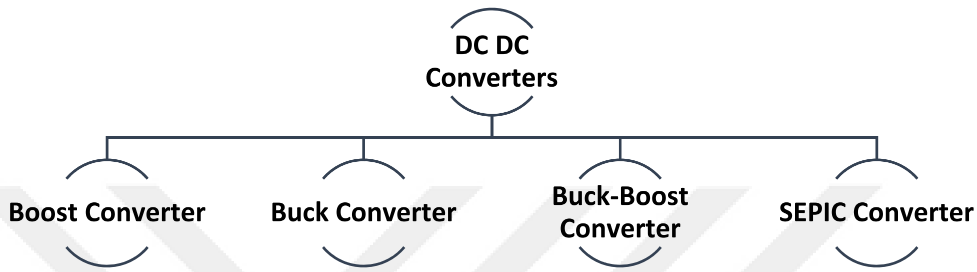

Figure 4.1. The most common types of DC-DC Converters implemented for MPPT of PV Systems

4.1.1. Boost Converter

Boost converter gives a voltage to the output, greater than its input voltage. The boost in this converter is obtained by using an inductor before the transistor in the circuit topology. The circuit diagram of the boost converter is shown in Figure 4.2

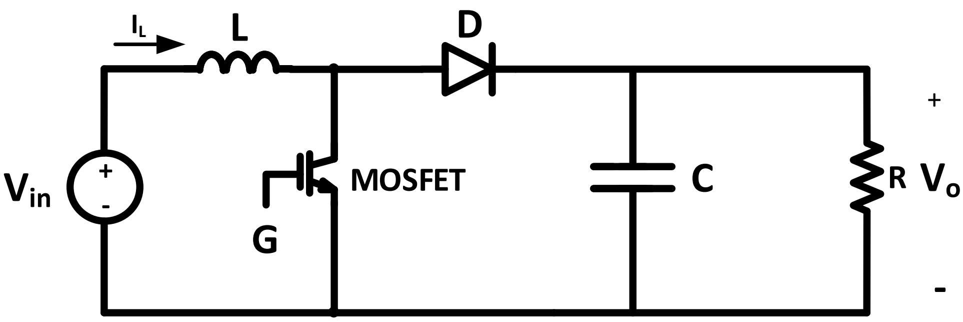

Figure 4.2. The circuit diagram of the boost converter

The relationship between the input and output voltage of the boost converter is given in Equation 4.1

$$V_0 = \frac{V_{in}}{1-D} \tag{4.1}$$

Where V_0 is the output voltage, V_{in} is the input voltage and D is the duty cycle of the PWM signal that drives the switching element in the circuit. The input current which is equal to the inductor current is shown in Equation 4.2.

$$I_L = I_{in} = \frac{V_0 \; x \; I_0}{V_{in}} = \frac{I_0}{(1-D)} = \frac{V_{in}}{(1-D)^2 \; x \; R} = \frac{V_0^2}{V_{in} \; x \; R} \tag{4.2}$$

Where $I_L$and I_{in} stand for inductor and input currents respectively. Equation 4.3 and Equation 4.4 shows the ripple currents I_{Lmin} and I_{Lmax} through the inductor.

$$I_{Lmin} = V_{in}\left(\frac{1}{Rx(1-D)^2} - \frac{DT}{2L}\right) \tag{4.3}$$

$$I_{Lmax} = V_{in}\left(\frac{1}{Rx(1-D)^2} + \frac{DT}{2L}\right) \tag{4.4}$$

Equation 4.5 shows the critical inductance value that is the border between continuous conduction mode and discontinuous conduction mode. When the inductance value of the circuit is greater than $L_{critical}$ ensures the boost in continuous conduction mode.

$$L_{critical} = \frac{D(1-D)^2 xR}{2f} \tag{4.5}$$

Where f stands for the electrical frequency. The formula for the output capacitor used for reducing the output voltage ripples is shown in Equation 4.6.

$$C = \frac{D}{Rx\left(\frac{\Delta V_0}{V_0}\right)xf} \tag{4.6}$$

4.1.2. Buck Converter

Buck converter is a nonisolated DC-DC converter that feeds the load connected to its terminals with an output voltage less than its input voltage. The circuit topology of this converter consists of a diode, an inductor, input and output capacitors and a switching element (MOSFET). The circuit diagram is shown in Figure 4.3.

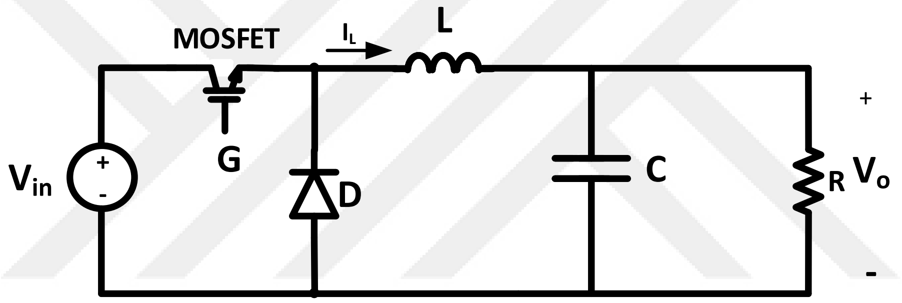

Figure 4.3. The circuit diagram of the boost converter

The relationship between input and output voltages is shown in Equation 4.7.

$$(V_{in} - V_0)DT + (-V_0)(1 - D)T = 0 \tag{4.7}$$

Where T is the period and D is the duty cycle. The simplified form of Equation 4.8 is shown in Equation 4.6.

$$V_0 = (D)V_{in} \tag{4.8}$$

Equations 3.9 and 3.10 show the ripple currents I_{Lmin} and I_{Lmax} through the inductor.

$$I_{Lmin} = DV_{in}\left(\frac{1}{R} - \frac{(1-D)T}{2L}\right) \tag{4.9}$$

$$I_{Lmax} = DV_{in}\left(\frac{1}{R} + \frac{(1-D)T}{2L}\right) \tag{4.10}$$

Equation 4.11 shows the critical inductor value that is the border between continuous conduction mode and discontinuous conduction mode.

$$L_{critical} = \left(\frac{1-D}{2}\right)TR \tag{4.11}$$

The greater values than $L_{critical}$ means the operation of converter in continuous current mode. The lesser values than $L_{critical}$ means the operation of the converter in discontinuous current mode. The equation of the output capacitor is shown in Equation 4.12.

$$C = \frac{1-D}{8L\left(\frac{\Delta V_0}{V_0}\right) f^2} \tag{4.12}$$

4.1.3. Buck-boost Converter

Buck-boost converter is a type of DC-DC converter that boosts or bucks the input voltage depending on the PWM signal at the gate terminal of the switching element. If the duty cycle of the PWM signal is greater than 0.5 the converter is in boost mode if it is less than 0.5 the converter is in buck mode. The circuit diagram of the Buck-boost converter is shown in Figure 4.4.

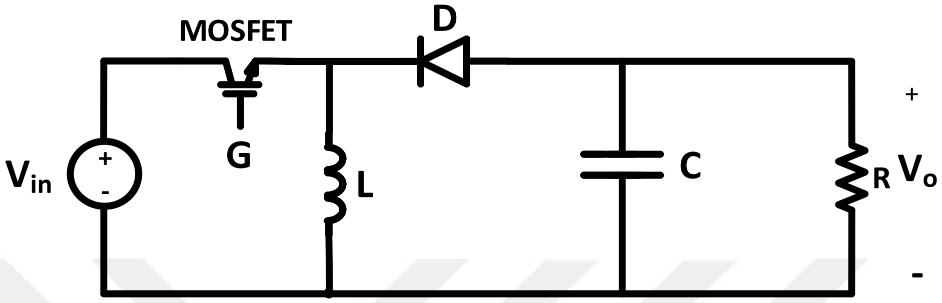

Figure 4.4. The circuit diagram of the buck-boost converter

The relationship between input and output voltages of the buck-boost converter is expressed in Equation 4.13.

$$\frac{V_0}{V_{in}} = \frac{D}{1-D} \tag{4.13}$$

The maximum and minimum currents flow through the inductor is expressed in Equations 3.14 and 3.15 respectively.

$$I_{lmax} = V_{in}\left[\frac{D}{R(1-D)^2} + \frac{DT}{2L}\right] \tag{4.14}$$

$$I_{lmin} = V_{in}\left[\frac{D}{R(1-D)^2} - \frac{DT}{2L}\right] \tag{4.15}$$

The capacitance of the output capacitor that is used for eliminating ripples is expressed in Equation 4.16.

$$C = \frac{D}{R\ x\ \left(\frac{\Delta V_0}{V_0}\right) x\ f} \tag{4.16}$$

4.1.4. SEPIC Converter

The main problem of basic DC-DC converters is their high current ripples that generate harmonics. Generally, LC filter is used to compensate these harmonic components. One of the drawbacks of using buck-boost converter is the voltage polarity reversing property of this converter. This condition may lead to overheating or failure of load devices. The implementation of the SEPIC overcomes both of abovementioned problems.

Single-ended primary-inductor converter (SEPIC) is a type of dc-dc converter that bucks or boosts its input voltage depending on the PWM signal at the gate terminal of the switching element. The circuit topology of SEPIC is shown in Figure 4.5.

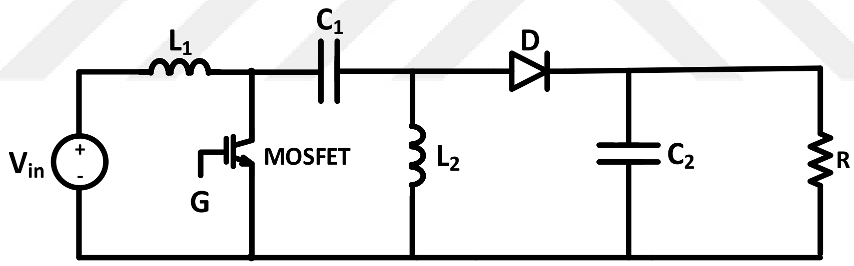

Figure 4.5. The circuit diagram of the SEPIC converter

SEPIC converter feeds the load with low harmonics and positive regulated voltage greater or less than its input voltage. The relationship between input and output voltages of SEPIC is shown in Equation 4.17.

$$V_0 = V_{in}\left(\frac{D}{1-D}\right) \tag{4.17}$$

The change in inductor current 1 (current on L1) is expressed in Equation 4.18.

$$\Delta i_1 = \frac{V_s DT}{L_i} = \frac{V_s D}{L_i f} \tag{4.18}$$

4.2. Maximum Power Point Tracking

The PV source impedance is variable depending on the environmental parameters such as temperature and solar irradiation. Since the fundamental law of the circuit, the theory suggests that the maximum power transfer occurs when the resistance of the load is equal to the resistance of the source. At this point, matching the impedance of the PV side with the impedance of the load side is required. This process is called the maximum power point tracking (MPPT). The variable impedance is provided by the DC-DC converter between the PV and the load. When the boost converter has used the relationship between the PV side and load side equivalent resistances is shown in Equation 4.19.

$$R_{eq} = R_{in}(1-d)^2 \tag{4.19}$$

Where R_{eq} is the equivalent resistance of seen from the PV side and R_{in} is the equivalent resistance of PV source. d is the duty cycle of the PWM signal that drives the switching element in the DC-DC converter. Figure 4.6 shows the block diagram of a PV system that comprises a PV array, MPPT controller, power converter and the load.

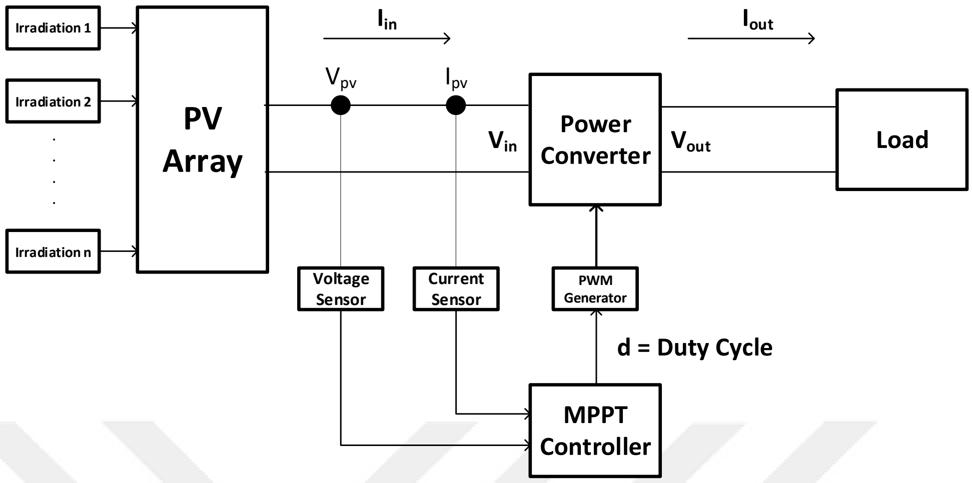

Figure 4.6. The block diagram of the PV system

In Chapter 2 various MPPT algorithms implemented for the PV systems under PSC are presented. In this section MPPT algorithms that are implemented in this thesis will be discussed in detail.

4.2.1. Particle Swarm Optimization (PSO)

PSO is a metaheuristic optimization algorithm implemented for MPPT of PV systems in the recent literature. (Dileep and Singh, 2017; Sundareswaran et al., 2015) The algorithm is based on the food search behavior of a flock of birds. The birds change their direction depending on their best location themselves and the best location of all. The position of a particle is given in Equation 4.20.

$$X_i^{k+1} = X_i^k + V_i^{k+1} \tag{4.20}$$

Where V_i^{k+1} stands for the velocity. It is expressed as in Equation 4.21.

$$V_i^{k+1} = WV_i^k + c_1 r_1 [p_{best} - X_i^k] + c_2 r_2 [G_{best} - x_i^k] \tag{4.21}$$

Where c_1 and c_2 are weights, r_1 and r_2 are random numbers from the interval (0,1), P_{best} is the best position of a particle, g_{best} is the best position of all particles and w is inertia constant. The movement of particles in the PSO algorithm is illustrated in Figure 4.7.

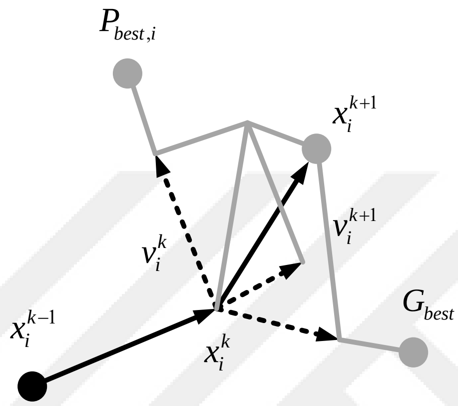

Figure 4.7. An illustration of the movement of particles in the PSO algorithm (Sameeullah and Swarup, 2016)

The flowchart of the PSO algorithm is shown in Figure 4.8. The main advantage of PSO in the context of PV systems is its independence of the shape of the Power-Voltage curve. Thus PSO is able to converge the global maximum power point (GMPP) under PSC. On the other hand, the main drawback of the PSO algorithm is its slow convergence speed that will directly affect the performance of the PV system. To overcome this problem many different hybrid algorithms are implemented with PSO in the recent literature. (Dileep and Singh, 2017; Sundareswaran et al., 2015)

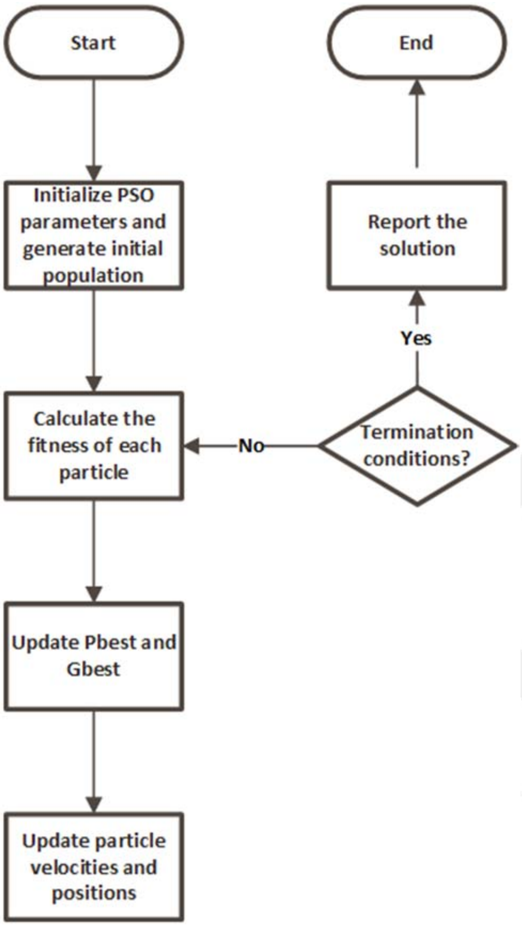

Figure 4.8. The Flowchart of the PSO Algorithm (Demirdelen et al., 2019)

4.2.2. Gravitational Search Algorithm (GSA)

GSA is an optimization algorithm that is based on Newton's gravitational theory. In this algorithm, every candidate solution i.e. agents has its mass proportional to its fitness function. At each generation, agents attract each other with a force that is proportional to their masses i.e. fitness function. Heavier mass means, heavier attraction force. Thus, better fitness function means higher attraction. The movement of an agent in the next iteration depends on the forces applied by other agents.

In the initialization phase, the masses of agents are randomly distributed and each of them is a potential solution. After the initialization phase, a velocity for each agent is defined. Next, forces on each agent and accelerations are calculated by using corresponding equations. At last, the positions are calculated. Equation 4.22 shows the gravitational force.

$$F = G\frac{M_1 M_2}{R^2} \tag{4.22}$$

Where G stands for the gravitational constant, R stands for the distance between the two particles, M_1 and M_2 stand for masses of the agents. Equation 4.23 shows the acceleration.

$$a = \frac{F}{M} \tag{4.23}$$

By using Equations 4.22 and 4.23 the position and velocity of agents can be calculated as in Equation 4.24 and 4.25 respectively.

$$d_i^{k+1} = d_i^k + \Phi_i^{k+1} \tag{4.24}$$

$$\Phi_i^{k+1} = X_i \Phi_i^k + a_i^{k+1} \tag{4.25}$$

Where X_i is a random variable from the interval [0,1]. The flowchart of the GSA algorithm is shown in Figure 4.9.

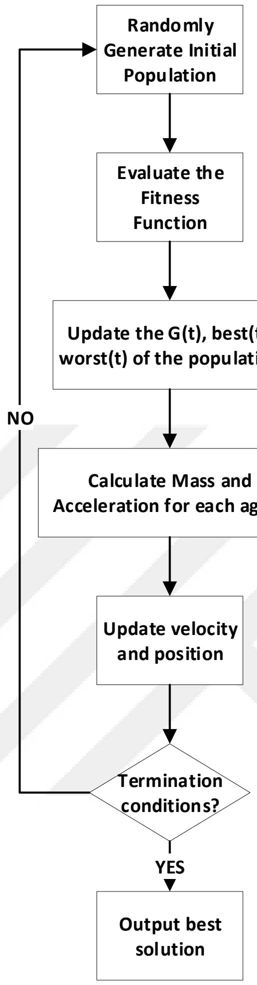

Figure 4.9. The Flowchart of the GSA Algorithm (Barisal et al., 2012)

4.2.3. Hybrid PSO-GSA Algorithm

The purpose of hybridization of PSO and GSA algorithms is to unite the social intelligence ability of PSO algorithm with local search ability of GSA algorithm. In this hybrid algorithm, the initialization of agents is a random process. After the initialization phase fitness function of all agents is determined. Next, gravitational constant, gravitational force and forces on all agents are calculated. By doing so, the agents with better solution i.e. with heavier mass attract other agents in the search space. Next, the acceleration values of agents are calculated. This phase ensures that the agents near the optimal solution move slower than others. After each iteration, the optimum solution until that iteration is updated. After that velocity and position data of agents are updated. Equation 4.25 of GSA algorithm is modified as Equation 4.26 in this hybrid algorithm.

$$\Phi_i^{k+1} = w\Phi_i^k + c_1 r_1 \; x \; a_i^k + c_2 r_2 [G_{best} - d_i^k] \tag{4.26}$$

Where c_1 and c_2 stand for acceleration coefficients, w is the inertia weight, G_{best} is the best position of agents, r_1 and r_2 are random numbers. Equation 4.27 shows the acceleration of the i_{th} agent at the k_{th} iteration.

$$a_i^k(t) = \frac{F_i\,(t)}{M_i(t)} \tag{4.27}$$

Calculation of mass is shown in Equation 4.28

$$M_i(t) = \frac{q_i(t)\; x \; 5}{\sum_{j=1}^{n} q_j(t)} \tag{4.28}$$

Where qi(t) stands for the strength of mass i at time t. qi(t), w(t) and b(t) are shown in Equations 4.29,4.30 and 4.31 respectively.

$$q_i(t) = \frac{f_i(t) - 0.99 \; x \; w(t)}{b(t) - w(t)} \tag{4.29}$$

$$b(t) = \min(f_i) \tag{4.30}$$

$$w(t) = \max(f_i)$$

(4.31)

Where f_i is the fitness function. The position update of particles is shown in Equation 4.32.

$$d_i^{k+1} = d_i^k + \Phi_i^{k+1} \tag{4.32}$$

The flowchart of the hybrid PSO-GSA algorithm is shown in Figure 4.10.

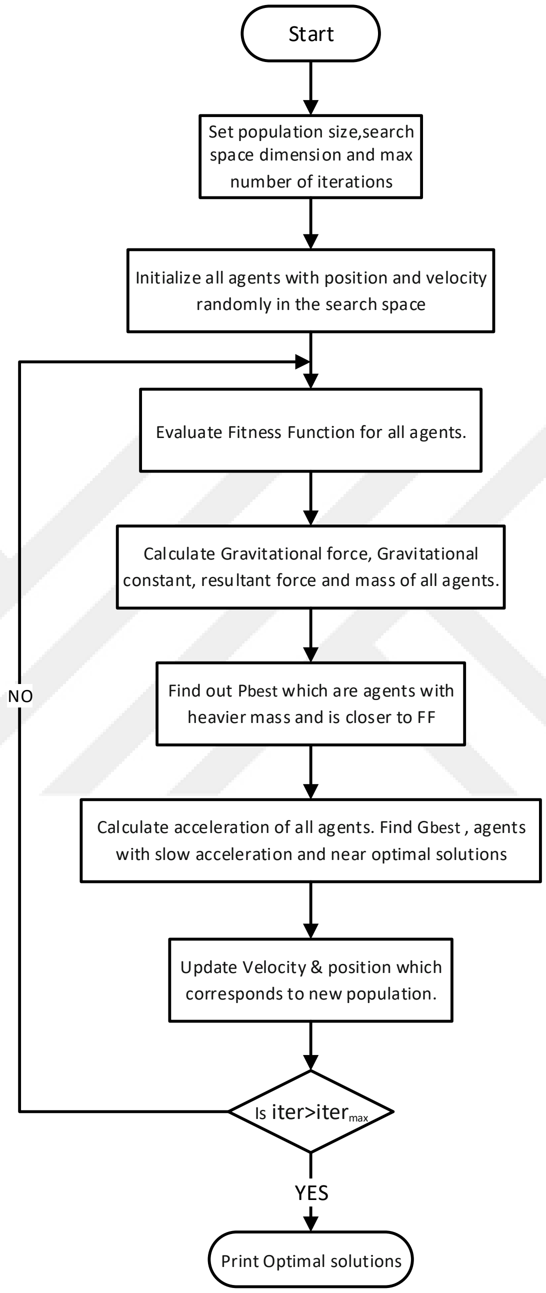

Figure 4.10. The Flowchart of the PSO-GSA Algorithm (Mangaiyarkarasi and Raja, 2014)

4.2.4. Grey Wolf Optimization Algorithm (GWO)

GWO is an optimization algorithm that is inspired by the behavior and hierarchy in the pack of grey wolves. These wolves are categorized into 4 groups namely alpha(α), beta(β), delta(δ) and omega(ω) wolves. These categories are associated with the social hierarchy of the grey wolves. Besides the social hierarchy of grey wolves, another social behavior of these wolves is group hunting. The main phases of group hunting are given in Figure 4.11 and corresponding photos of these phases are shown in Figure 4.12.

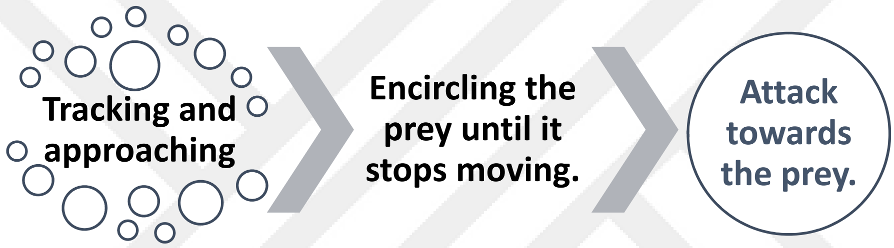

Figure 4.11. The main phases of grey wolf hunting (Mirjalili et al., 2014)

Figure 4.12. Phases of Grey Wolf hunting: (A) Tracking, (B) Approaching, (C)-(D) Encircling, (E) Attack (Muro et al., 2011)

In GWO algorithm the best solution is called the alpha. Second and third best solutions are beta and delta. The remaining solutions are called omega. The encircling phase of the attack of grey wolves is expressed as in Equations 4.33 and 4.34.

$$\vec{D} = |\vec{C}\,.\vec{X}_p(t) - \vec{X}_p(t)| \tag{4.33}$$

$$\vec{X}(t+1) = \vec{X}_p(t) - \vec{A}.\vec{D} \tag{4.34}$$

Where t stands for the iteration number D, A, and C are coefficient vectors, X is the position vector of grey wolves and X_p is the position vector of the prey. A and C vectors are calculated as in equations 4.35 and 4.36.

$$\vec{A} = 2\vec{a}\,.\vec{r_1} - \vec{a} \tag{4.35}$$

$$\vec{C} = 2.\vec{r}_2 \tag{4.36}$$

Where r_1 and r_2 stand for random vectors from the interval [0,1]. The hunting behavior of a pack of grey wolves is shown in Equations 4.37, 4.38, 4.39.

$$\overrightarrow{D_\alpha} = \left|\overrightarrow{C_1}\,.\overrightarrow{X_\alpha} - \vec{X}\right|, \qquad \overrightarrow{D_\beta} = \left|\overrightarrow{C_2}\,.\overrightarrow{X_\beta} - \vec{X}\right|, \qquad \overrightarrow{D_\delta} = \left|\overrightarrow{C_3}\,.\overrightarrow{X_\delta} - \vec{X}\right| \tag{4.37}$$

$$\overrightarrow{X_1} = \overrightarrow{X_\alpha} - \overrightarrow{A_1}\,|\,.\left(\overrightarrow{D_\alpha}\right), \qquad \overrightarrow{X_2} = \overrightarrow{X_\beta} - \overrightarrow{A_2}\,|.\left(\overrightarrow{D_\beta}\right),$$
$$\overrightarrow{X_3} = \overrightarrow{X_\delta} - \overrightarrow{A_3}\,.\left(\overrightarrow{D_\delta}\right) \tag{4.38}$$

$$\vec{X}(t+1) = \frac{\overrightarrow{X_1} + \overrightarrow{X_2} + \overrightarrow{X_3}}{3} \tag{4.39}$$

The flowchart of the GWO algorithm is shown in Figure 4.13.

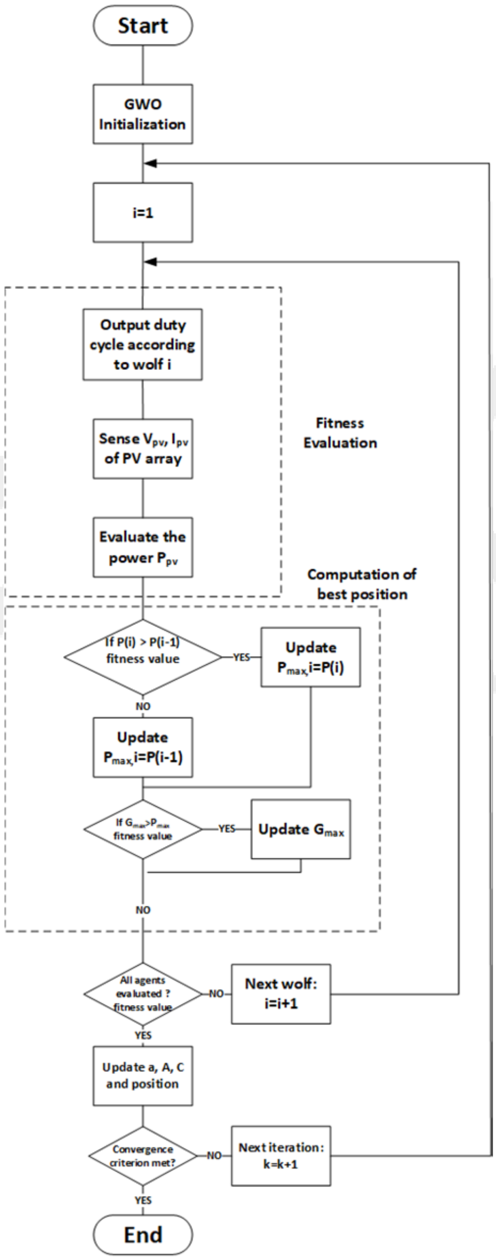

Figure 4.13. The flowchart of the GWO algorithm (Mohanty et al., 2016)

4.2.5. Butterfly Optimization Algorithm (BOA)

BOA is an optimization algorithm that mimics the food search behavior of butterflies. (Arora and Singh, 2019) In order to model the algorithm some of the biological features of butterflies will also be presented. For butterflies, the most important sense is the sense of smell because of its role in food searching for butterflies. Smell receptors of butterflies are their antennas, legs, and palps. These receptors also take part in finding a mating partner. It is known that butterflies can locate the source of a fragrance in their surrounding area. In the BOA butterflies are agents in the search space. Butterflies are generating fragrance with various intensities. When a butterfly in the search space changes its location, its fragrance intensity will also change. The fragrance of a butterfly propagates along with the search space. Hence, other butterflies can sense the location of it and will move toward it. This process is named as a global search in the BOA. If a butterfly cannot sense the fragrance of any other butterfly, it will move randomly. Two important parameters for the BOA are the location of a mating partner and the location of food. The three main characteristics of butterflies in BOA are as following:

1. All butterflies should have a fragrance to attract other butterflies in the search space.
2. Butterflies in the search space should change their position randomly or towards the butterfly with the maximum fragrance.
3. The landscape of the objective function will determine the stimulus intensity of butterflies.

BOA can be divided into 3 phases namely; initialization, iteration, and final phase. The algorithm starts from the initialization phase at each run. After the initialization phase iterations start for the search of the optimum solution. Next, when the optimum solution is found the final phase will start to output the best solution found.

In the start of the first phase, the solution space and the objective function should be determined. Next, initial values assigned to the parameters in the algorithm. After that, the population of butterflies is created. Next, the agents are randomly distributed in the search space. The fitness and fragrance values of agents also calculated.

In the iteration phase, the butterflies change their position and the fitness values are calculated for new positions. After that, the fragrance of butterflies is generated according to Equation 4.40.

$$f = cI^{a} \tag{4.40}$$

Where I is stimulus intensity, f is the fragrance, a is value depend on fragrance and c is the sensory modality. The algorithm consists of two main stages; Global and local search phases. Global search phase is shown in Equation 4.41.

$$x_i^{t+1} = x_i^t + \left(r^2 \text{ x } g^* - x_i^t\right) x\, f_i \tag{4.41}$$

Where x_i^t stands for the solution vector, g^* stands for the best solution in the current iteration, f_i is the fragrance of the ith butterfly and r is a random number. Local search phase is shown in Equation 4.42.

$$x_i^{t+1} = x_i^t + \left(r^2 \text{ x } x_j^t - x_i^t\right) x\, f_i \tag{4.42}$$

Where x_i^t and x_k^t stands for ith and jth butterflies in the solution space, respectively. Until the stop criteria are satisfied the iteration process continues. The BOA is summarized in the pseudo-code shown in Figure 8.

```
Objective function f(x), x=(x1, x2, ..., xdim) , dim = no. of dimensions
Generate initial population of n Butterflies xi= (i=1, 2, ..., n)
Stimulus Intensity Ii at xi is determined by f(xi)
Define sensor modality c, power exponent a and switch probability p
while stopping criteria not met do
    for each butterfly bf in population do
            Calculate fragrance for bf
    end for
    Find the best bf
    for each butterfly bf in population do
            Generate a random number r from [0, 1]
            if r < p then
                    Move towards best butterfly/solution
            else
                    Move randomly using Eq. (3)
            end if
    end for
    Update the value of a
end while
Output the best solution found.
```

Figure 4.14. The pseudocode of BOA (Arora and Singh, 2019)

5. RESULTS AND DISCUSSION

The diagram of the proposed system is shown in Figure 5.1. Between the output of the PV array and the load, there is a DC-DC boost converter in order to implement MPPT algorithms. The whole system is modeled and simulated by using MATLAB/Simulink. Some of the characteristic parameters of the system are given in Table 5.1.

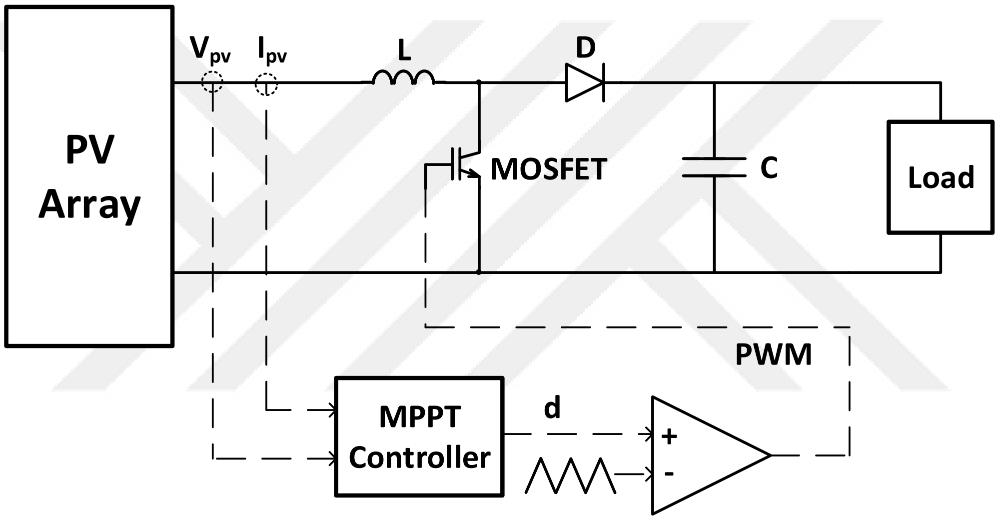

Figure 5.1. The use of the Boost converter for MPPT in the proposed system

Table 5.1. Parameters of the proposed system

Parameter	Value
PV Array Open Circuit Voltage	38 V
PV Array Short Circuit Current	8.8 A
Inductance (L)	1 mH
Capacitance (C)	50 mF
Load Resistance (R)	50 Ω
Switching Frequency	25 kHz

In this section, the performance analysis of the Hybrid PSO-GSA and GWO algorithms from the literature and proposed Butterfly Optimization MPPT algorithm is presented. In order to test the performance of the mentioned algorithms under uniform insolation and partial shading conditions. Three different insolation scenarios were created. These scenarios are shown in Figure 5.2.

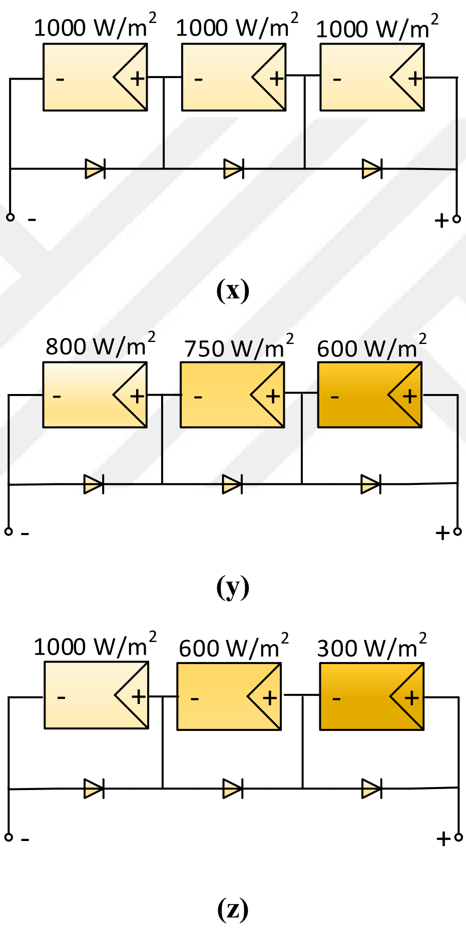

Figure 5.2. Insolation levels of PV panels in the array for different shading patterns

The Power-Voltage and Current-Voltage characteristics of PV system under insolation pattern x, y and z are shown in Figure 5.3 and Figure 5.4 respectively. It is seen from figures that the global maximum power point (GMPP) of PV system under insolation pattern x is 250 W, under insolation pattern y is 162.4 W and under insolation, pattern z is 104.5 W.

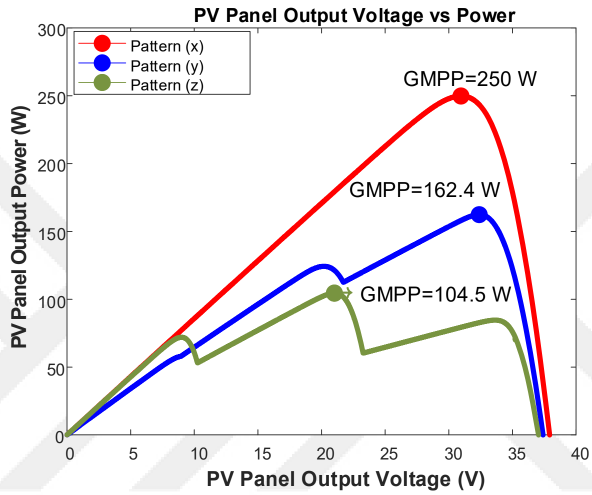

Figure 5.3. P-V characteristics of PV system under x,y, and z insolation patterns
,

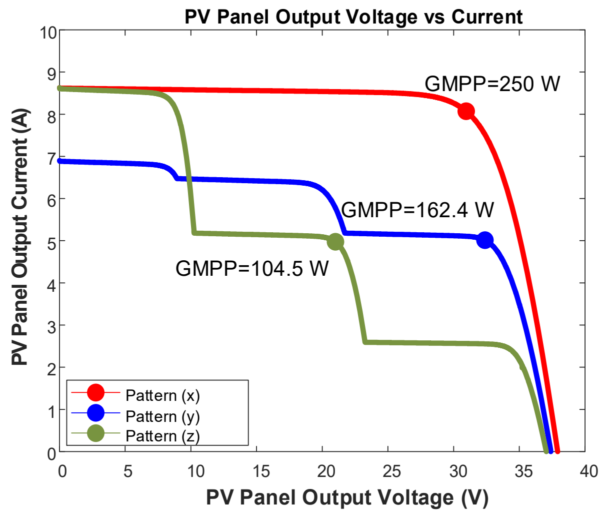

Figure 5.4. I-V characteristics of the PV system under x,y, and z insolation patterns

5.1. Case 1

In this section, the performance analysis of PSO-GSA, GWO, and BOA algorithms under insolation pattern x is presented. Figures 5.5, 5.6, 5.7 and 5.8 show the resulting graphs of PSO-GSA MPPT method, Figures 5.9, 5.10, 5.11 and 5.12 show the resulting graphs of GWO MPPT method, Figures 5.13, 5.14, 5.15 and 5.16 show the resulting graphs of BOA MPPT method under insolation pattern x.

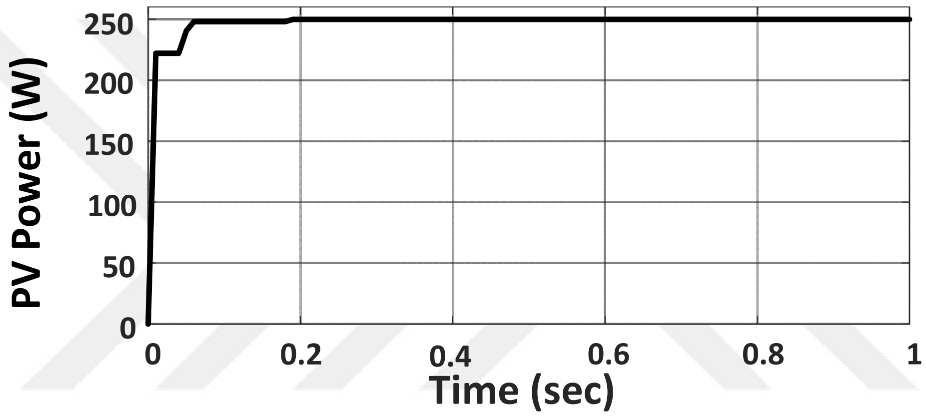

Figure 5.5 Graph of PV power for PSO-GSA algorithm under insolation pattern x

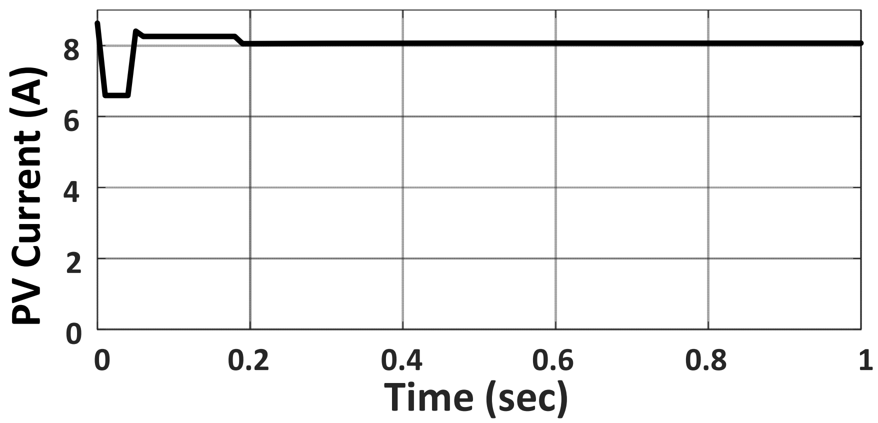

Figure 5.6. Graph of PV current for PSO-GSA algorithm under insolation pattern x

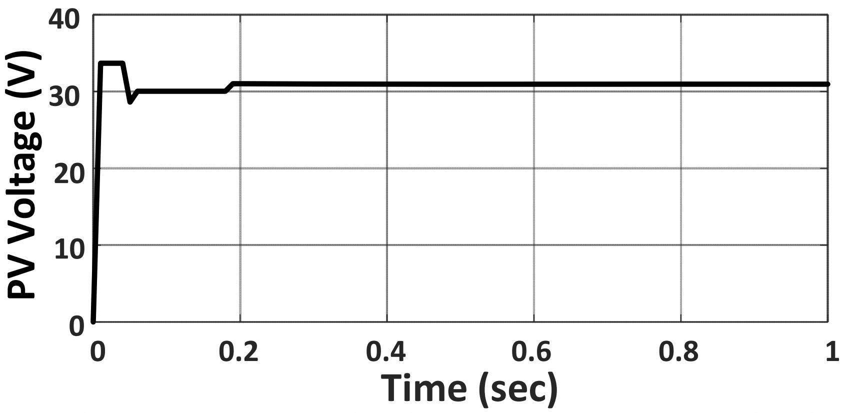

Figure 5.7. Graph of PV Voltage for PSO-GSA algorithm under insolation pattern x

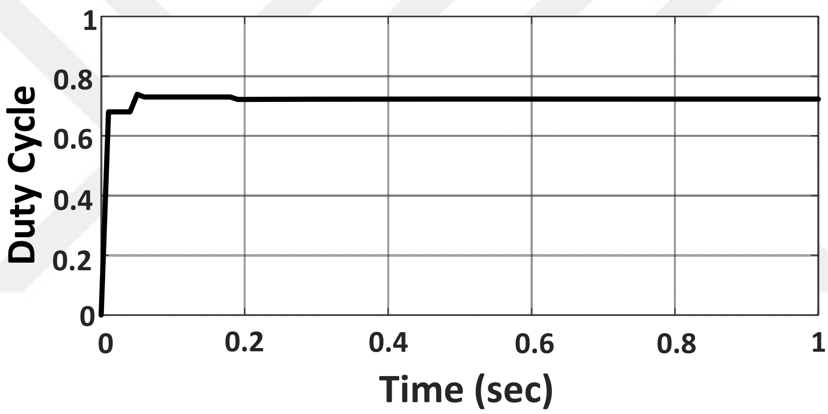

Figure 5.8. Graph of Duty Cycle for PSO-GSA algorithm under insolation pattern x

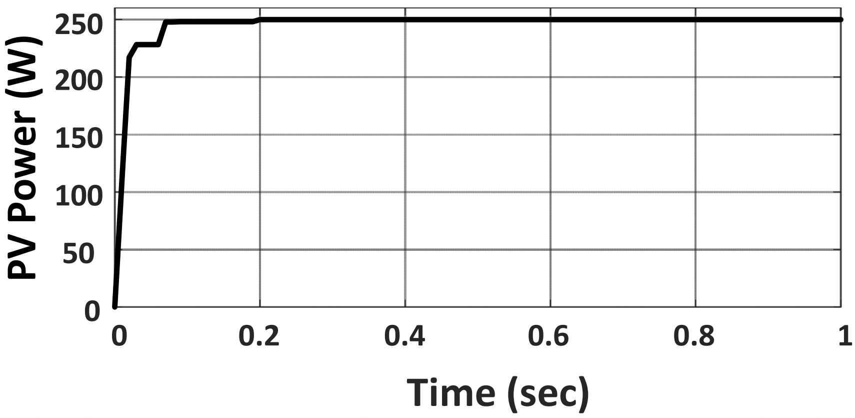

Figure 5.9. Graph of PV Power for GWO algorithm under insolation pattern x

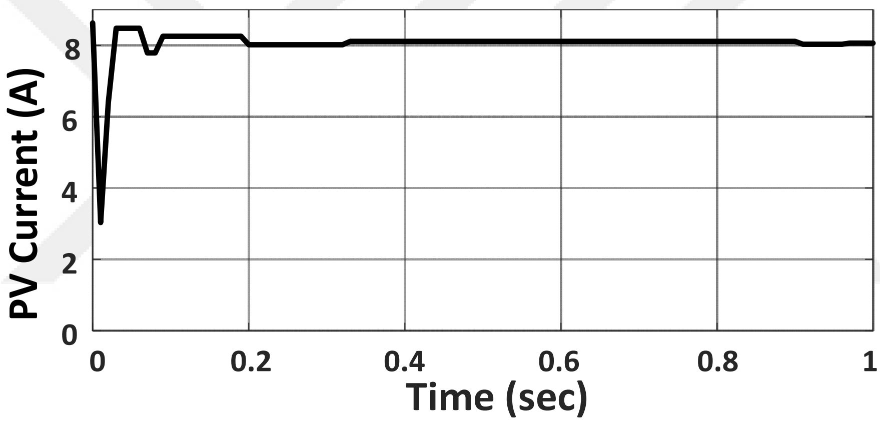

Figure 5.10. Graph of PV Current for GWO algorithm under insolation pattern x

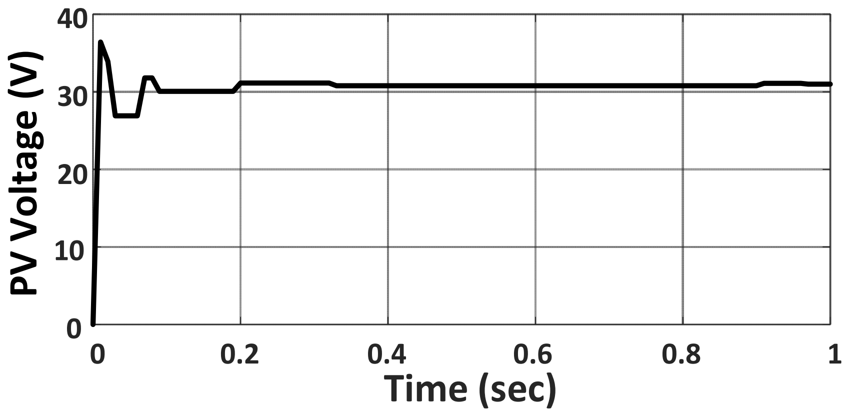

Figure 5.11. Graph of PV Voltage for GWO algorithm under insolation pattern x

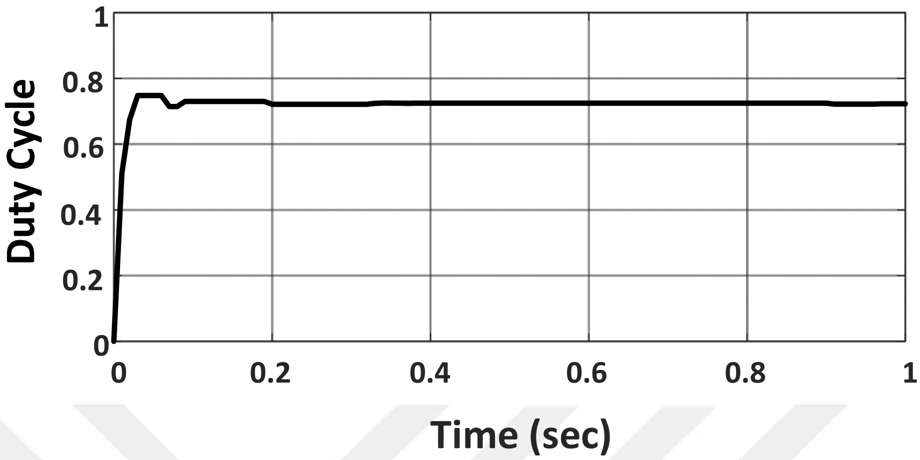

Figure 5.12. Graph of Duty Cycle for GWO algorithm under insolation pattern x

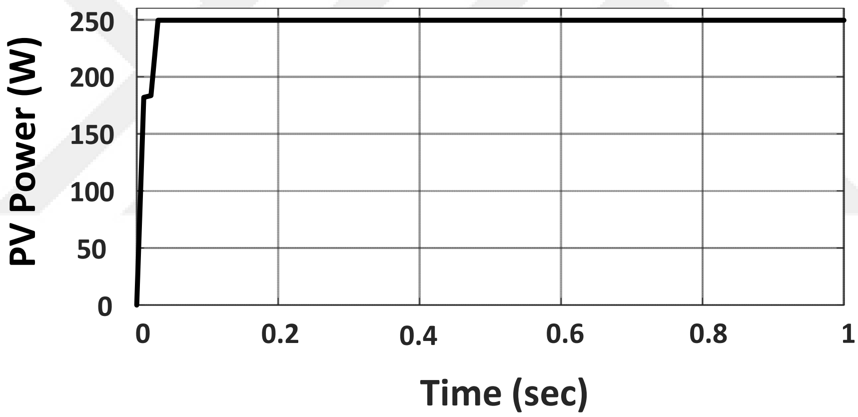

Figure 5.13. Graph of PV Power for BOA under insolation pattern x

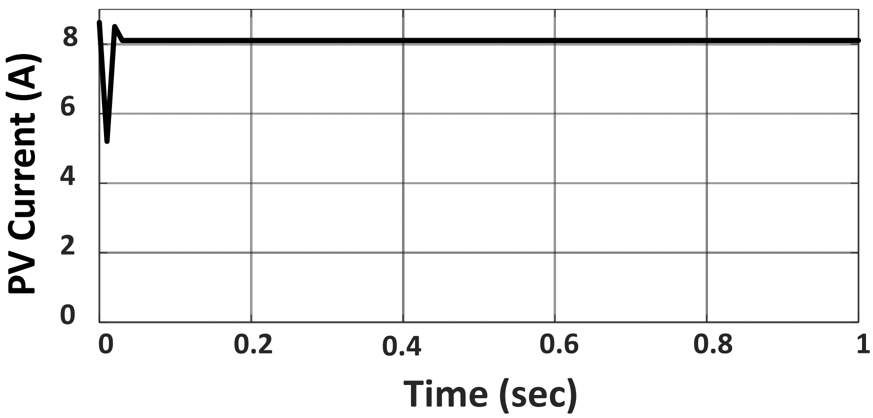

Figure 5.14. Graph of PV Current for BOA under insolation pattern x

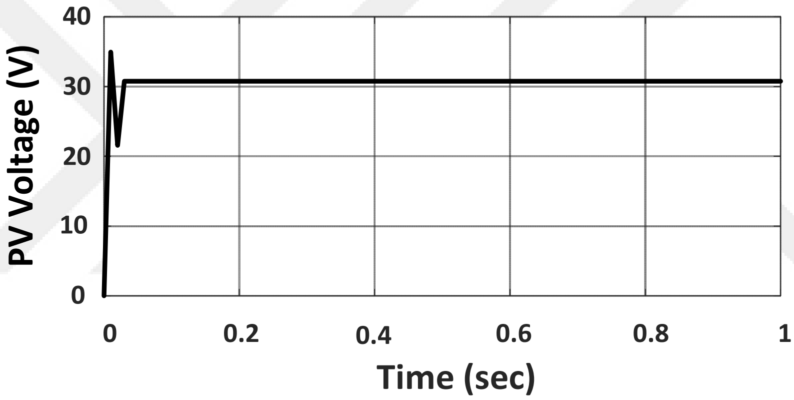

Figure 5.15 Graph of PV Voltage for BOA under insolation pattern x

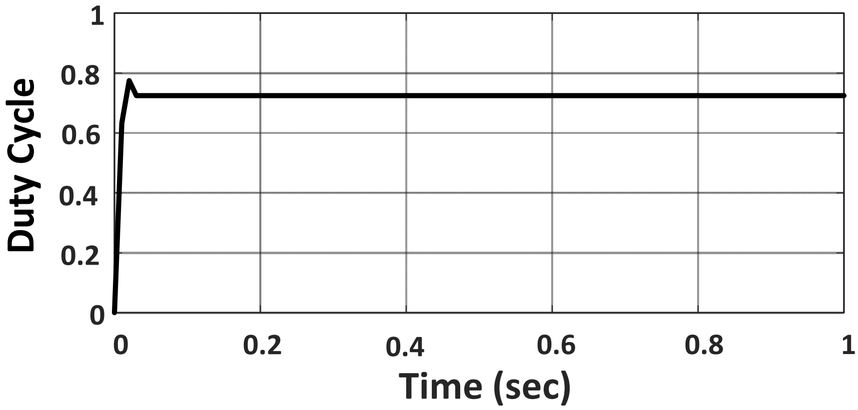

Figure 5.16 Graph of Duty Cycle for BOA under insolation pattern x

Under insolation pattern X, all the three algorithms converge to the GMPP that is at 250 W. However, when the convergence speeds of the algorithms are examined, it is seen that PSO-GSA converged to the GMPP after 0.12 s, GWO converged after 0.11 s and BOA converged after 0.07 s. So, for insolation pattern x, BOA is %36.36 faster than GWO and %41.66 faster than PSO-GSA.

5.2. Case 2

In this section, the performance analysis of PSO-GSA, GWO and BOA algorithms under insolation pattern y is presented. Figures 5.17, 5.18, 5.19 and 5.20 show the resulting graphs of PSO-GSA MPPT method, Figures 5.21, 5.22, 5.23 and 5.24 show the resulting graphs of GWO MPPT method, Figures 5.25, 5.26, 5.27 and 5.28 show the resulting graphs of BOA MPPT method under insolation pattern y.

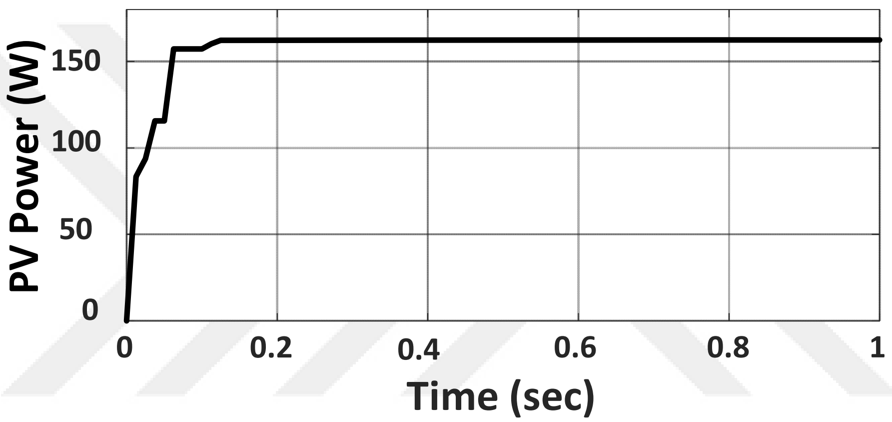

Figure 5.17. Graph of PV Power for PSO-GSA under insolation pattern y

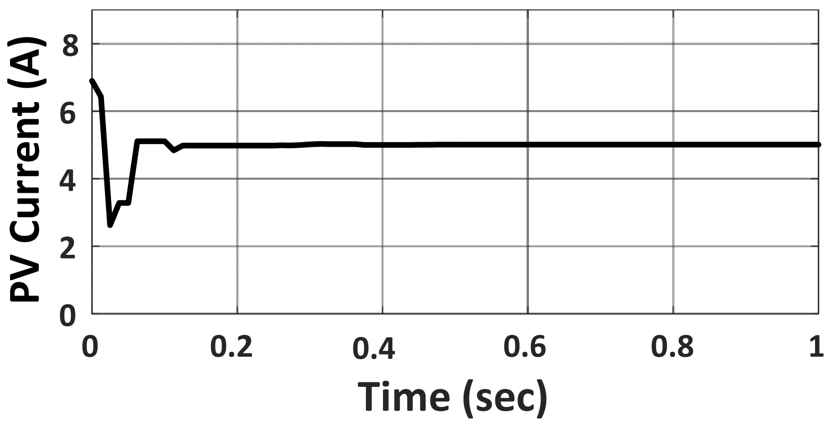

Figure 5.18. Graph of PV Current for PSO-GSA under insolation pattern y

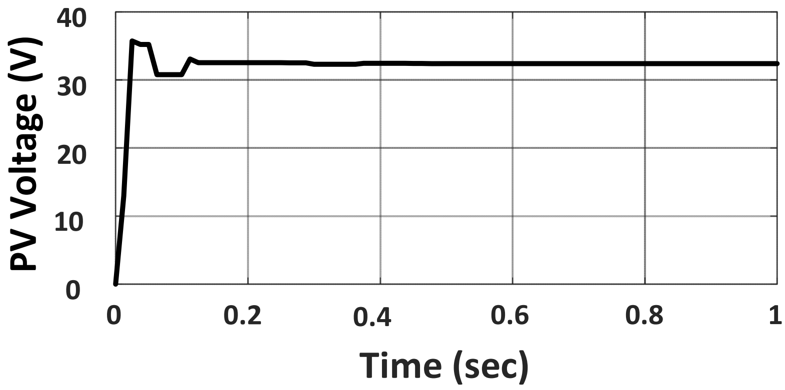

Figure 5.19. Graph of PV Voltage for PSO-GSA under insolation pattern y

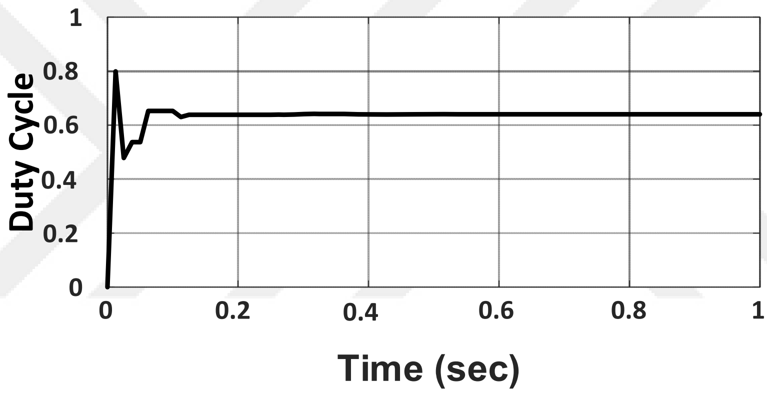

Figure 5.20. Graph of Duty Cycle for PSO-GSA under insolation pattern y

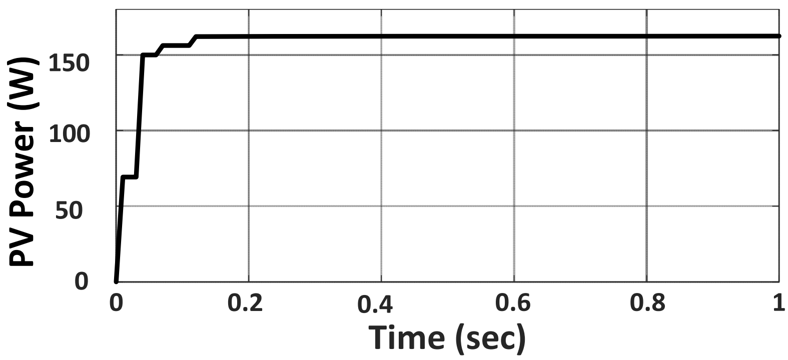

Figure 5.21. Graph of PV Power for GWO Algorithm under insolation pattern y

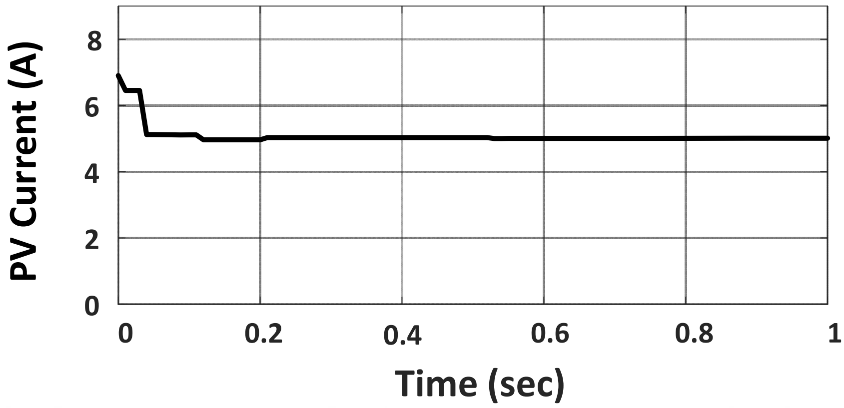

Figure 5.22. Graph of PV Current for GWO Algorithm under insolation pattern y

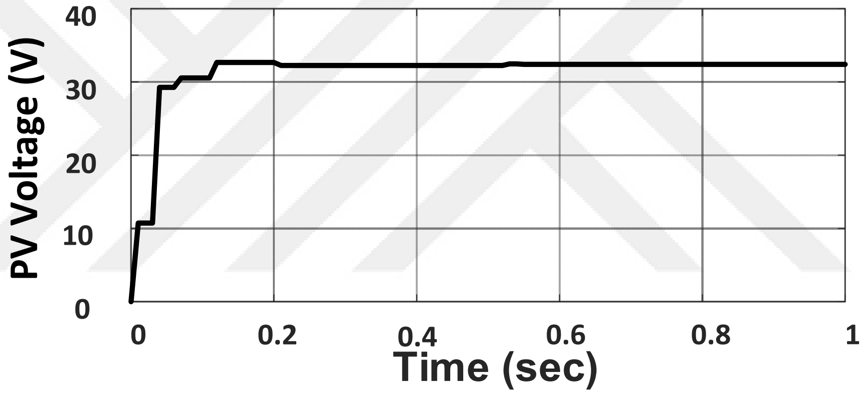

Figure 5.23. Graph of PV Voltage for GWO Algorithm under insolation pattern y

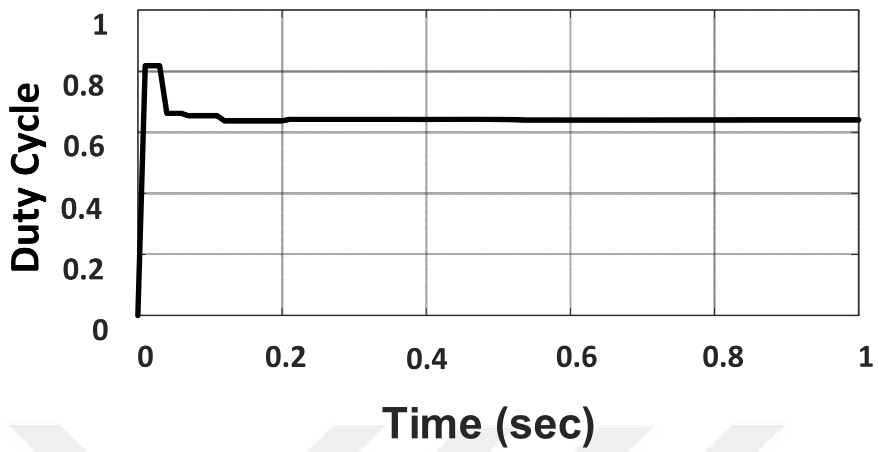

Figure 5.24. Graph of Duty Cycle for GWO Algorithm under insolation pattern y

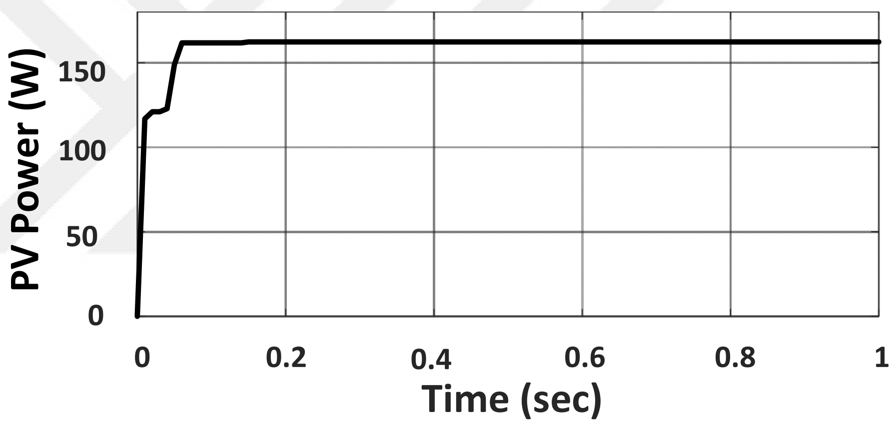

Figure 5.25. Graph of PV Power for BOA under insolation pattern y

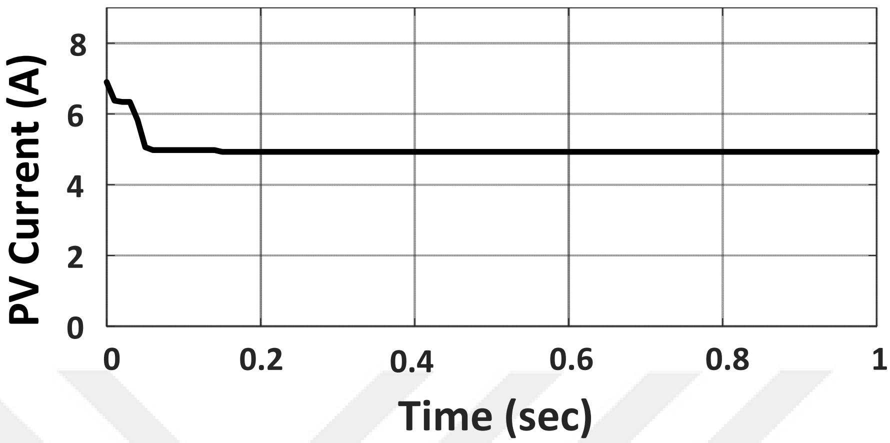

Figure 5.26. Graph of PV Current for BOA under insolation pattern y

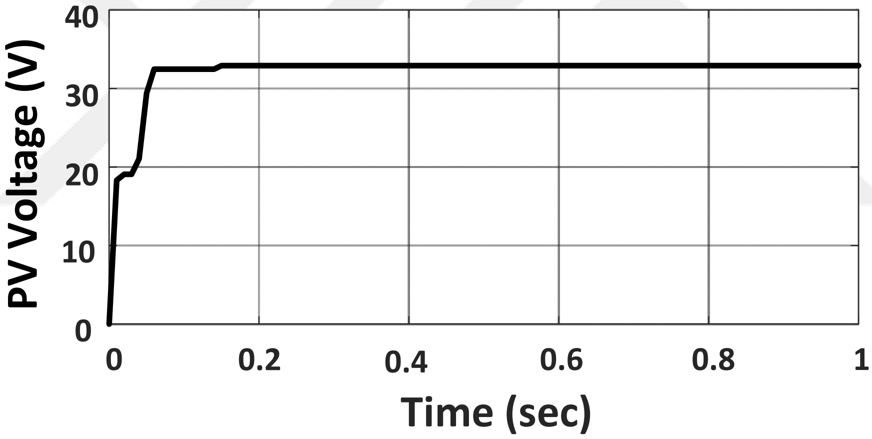

Figure 5.27. Graph of PV Voltage for BOA under insolation pattern y

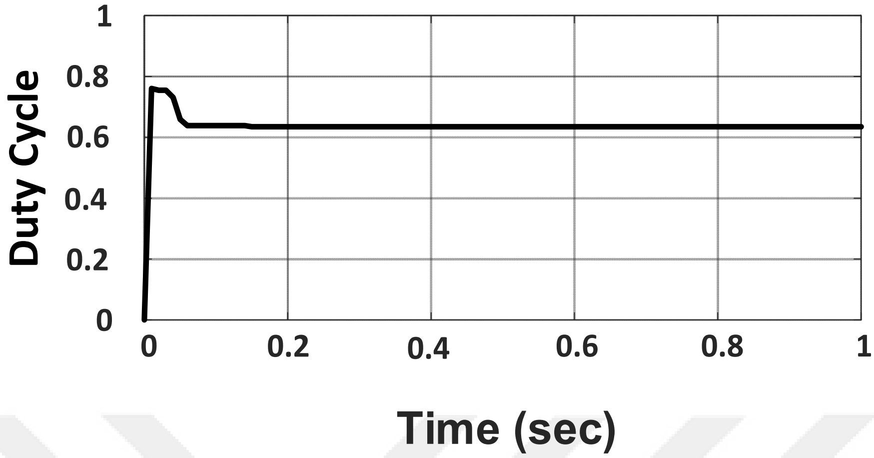

Figure 5.28. Graph of Duty Cycle for BOA under insolation pattern y

Under insolation pattern y, all the three algorithms converge to the GMPP that is at 162.4 W. However, when the convergence speeds of the algorithms are examined, it is seen that PSO-GSA converged to the GMPP after 0.16 s, GWO converged after 0.14 s and BOA converged after 0.1 s. So, for insolation pattern y, BOA is %28.57 faster than GWO and %37.5 faster than PSO-GSA.

5.3. Case 3

In this section, the performance analysis of PSO-GSA, GWO, and BOA algorithms under insolation pattern y are presented. Figures 5.29, 5.30, 5.31 and 5.32 show the resulting graphs of PSO-GSA MPPT method, Figures 5.33, 5.34, 5.35 and 5.36 show the resulting graphs of GWO MPPT method, Figures 5.37, 5.38, 5.39 and 5.40 show the resulting graphs of BOA MPPT method under insolation pattern z.

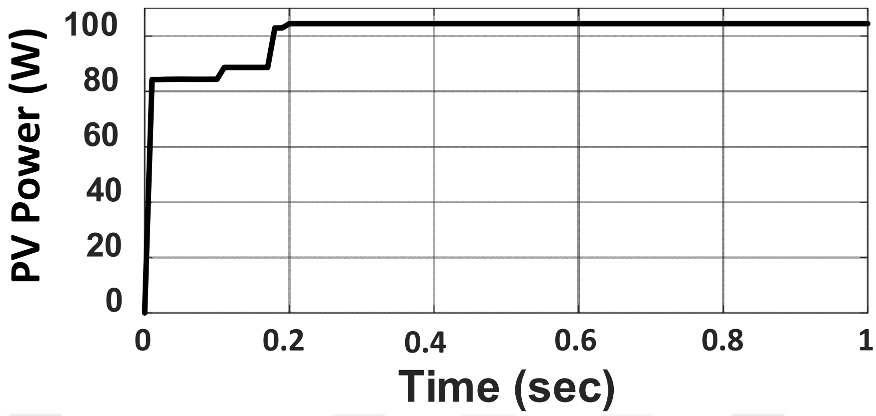

Figure 5.29. Graph of PV Power for PSO-GSA under insolation pattern z

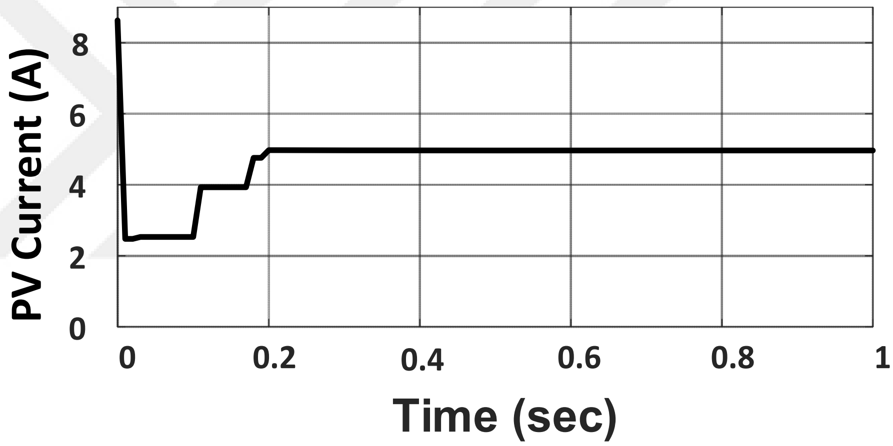

Figure 5.30. Graph of PV Current for PSO-GSA under insolation pattern z

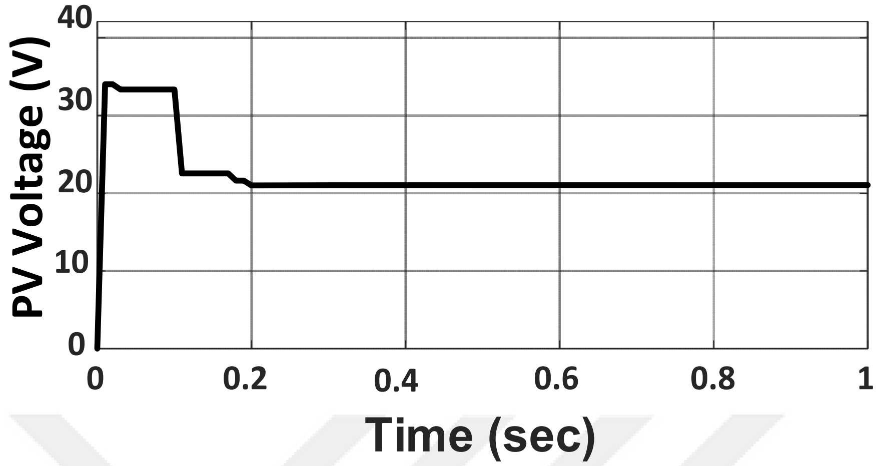

Figure 5.31. Graph of PV Voltage for PSO-GSA under insolation pattern z

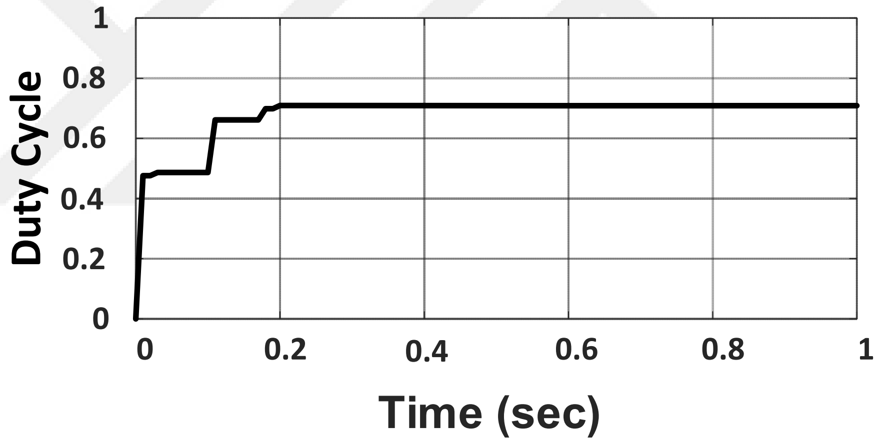

Figure 5.32. Graph of Duty Cycle for PSO-GSA under insolation pattern z

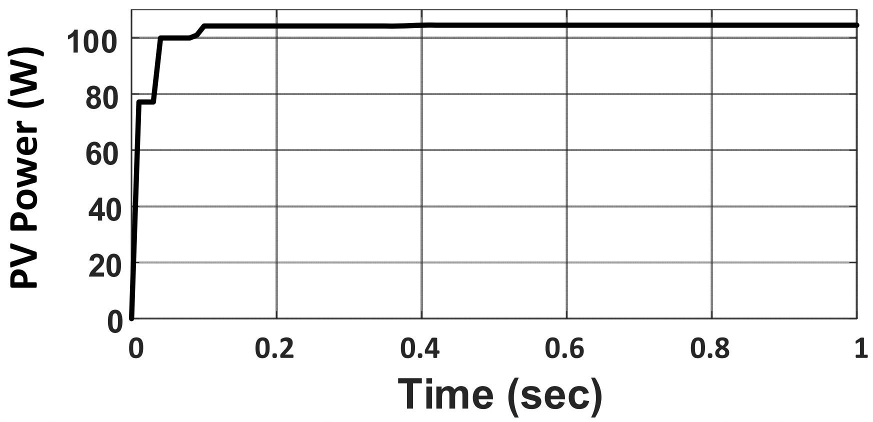

Figure 5.33. Graph of PV Power for GWO Algorithm under insolation pattern z

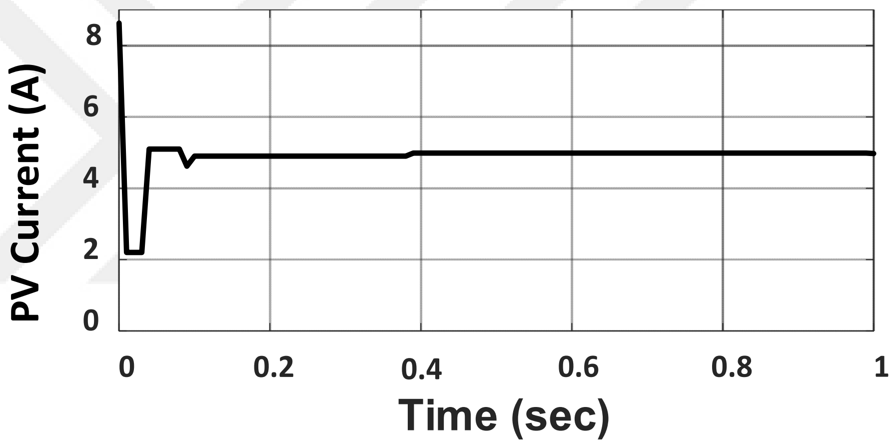

Figure 5.34. Graph of PV Current for GWO Algorithm under insolation pattern z

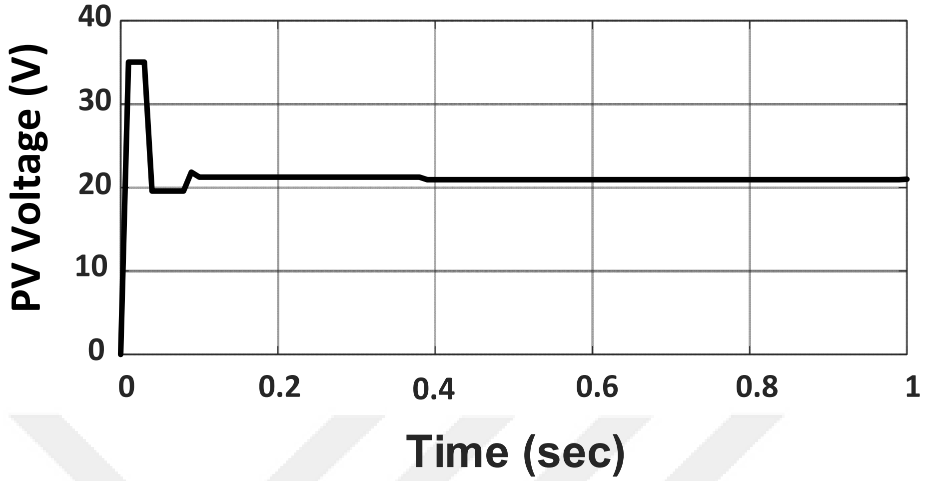

Figure 5.35. Graph of PV Voltage for GWO Algorithm under insolation pattern z

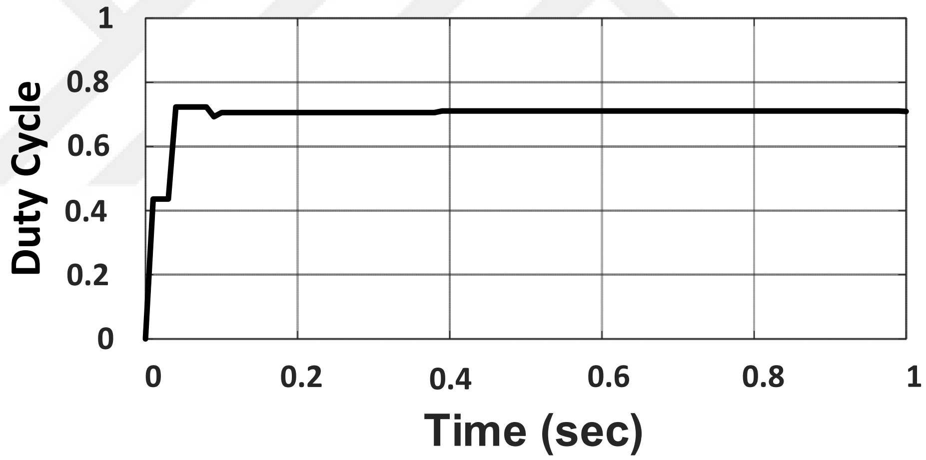

Figure 5.36. Graph of Duty Cycle for GWO Algorithm under insolation pattern z

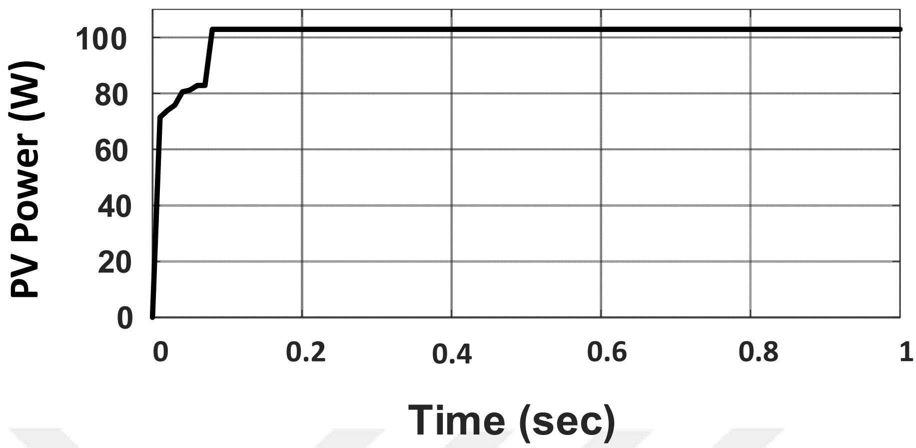

Figure 5.37. Graph of PV Power for BOA under insolation pattern z

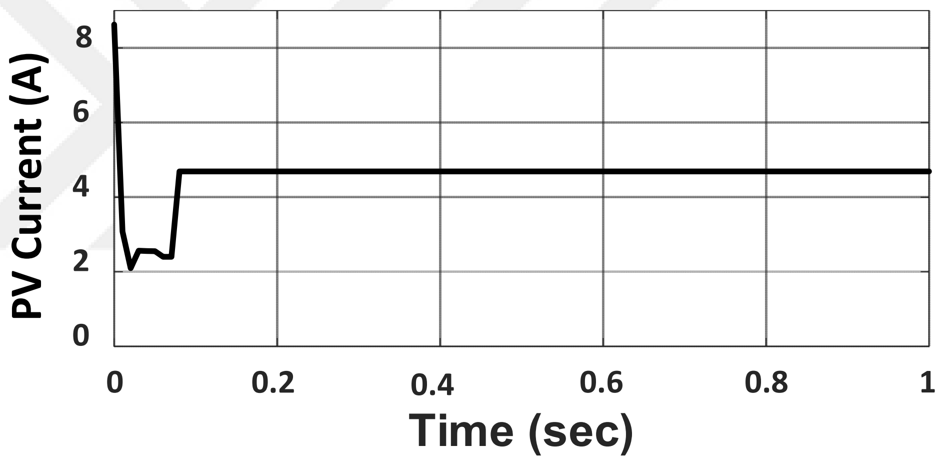

Figure 5.38. Graph of PV Current for BOA under insolation pattern z

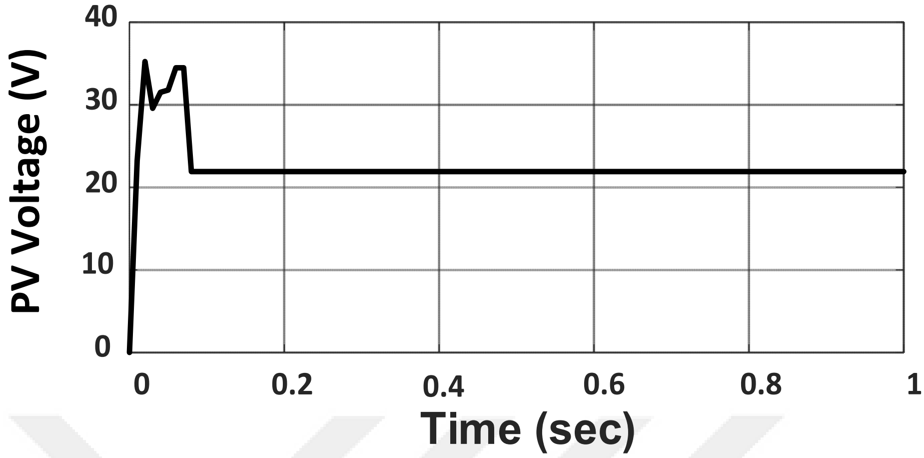

Figure 5.39. Graph of PV Voltage for BOA under insolation pattern z

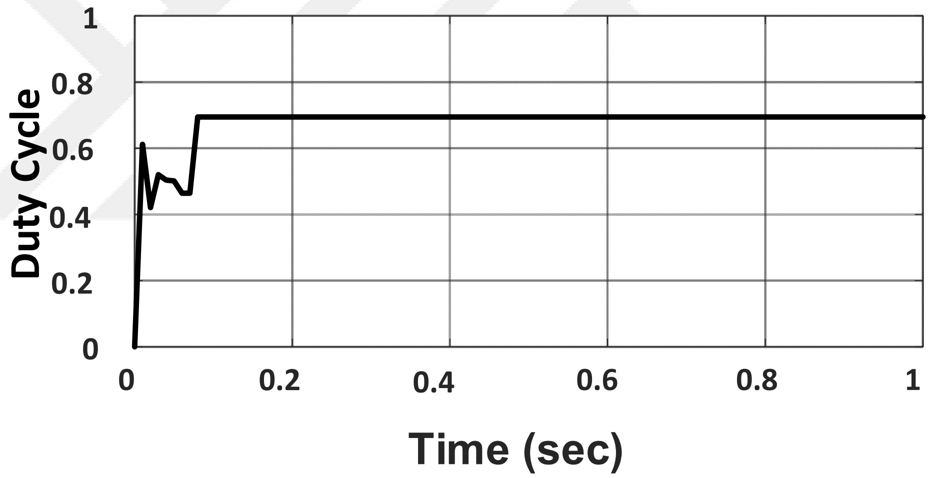

Figure 5.40. Graph of Duty Cycle for BOA under insolation pattern z

All of the algorithms converge to the GMPP that is at 104.5 W under insolation pattern z. However, when the convergence speeds of the algorithms are examined, it is seen that PSO-GSA converged to the GMPP after 0.21 s, GWO converged after 0.17 s and BOA converged after 0.1 s. So, for insolation pattern z, BOA is %52.38 faster than GWO and %41.17 faster than PSO-GSA

5.4. Summary of simulation scenarios

Performance analysis of PSO-GSA, GWO and BOA MPPT methods under three different insolation scenarios is given in previous pages. The summary of these results is given in Table 5.2. It is seen from the table that all three algorithms were able to trach the GMPP under every insolation scenario. However, the BOA MPPT method has the fastest convergence speed among all MPPT methods in all the three insolation scenarios.

Table 5.2. Summary of simulation scenarios

Shading Pattern	MPPT Algorithm	Power	Tracking Speed	GMPP
Pattern x	PSO-GSA	250 W	0.12 s	250 W
	GWO	250 W	0.11 s	
	BOA	250 W	0.07 s	
Pattern y	PSO-GSA	162.4 W	0.16 s	162.4 W
	GWO	162.4 W	0.14 s	
	BOA	162.4 W	0.10 s	
Pattern z	PSO-GSA	104.5 W	0.21 s	104.5 W
	GWO	104.5 W	0.17 s	
	BOA	104.5 W	0.10 s	

5.5. Statistical analysis of the proposed algorithms

In this section, a statistical evaluation of the results obtained from the simulation analysis of the PSO-GSA, GWO and proposed BOA methods are given. The statistical metrics used in this evaluation are; Standard Deviation (STD), Average Relative Error (RE), Mean Absolute Error (MAE) and Root Mean Square Error (RMSE). These metrics can be calculated as the following equations;

$$STD = \sqrt{\frac{\sum_{i=1}^{n_r}(P_{pvt} - \overline{P}_{pvt})}{n_r}} \tag{5.1}$$

$$RE = \frac{\sum_{i=1}^{n_r}(P_{PVe,i} - P_{pvt})}{P_{pvt}} * 100 \tag{5.2}$$

$$MAE = \frac{\sum_{i=1}^{n_r}(P_{PVe,i} - P_{pvt})}{n_r} \tag{5.3}$$

$$RMSE = \sqrt{\frac{\sum_{i=i}^{n_r}(P_{PVe,i} - P_{pvt})}{n_r}} \tag{5.4}$$

In the above equations, n_r stands for the number of runs of the model in MATLAB/SIMULINK. $P_{PVe,i}$ stands for the estimated PV power in the ith iteration and P_{pvt} is the true PV power obtained from the PV model in MATLAB/Simulink. To analyze the performances of the algorithms, all simulations have been executed 100 times. Tables 3-5 show the statistical performance analysis of BOA, PSO-GSA and GWO MPPT method under 3 different partial shading patterns respectively. STD values in Tables 5.3, 5.4 and 5.5 show that there is not any major change in the results during the iterations. I.e. the algorithms have stable operation while finding GMPP. Table 5.6 summarized the statistical analysis of the algorithms, Table 7 compares parameters such as efficiency, convergence speed and the number of iterations of the algorithms. It is seen from Table 5.6 and Table 5.7 that the BOA method has the highest efficiency and fastest convergence speed to the GMPP among the algorithms implemented in this study.

Table 5.3. Statistical Performance Evaluation of BOA

Pattern	Global	Best	Worst	Average	Median	STD	RE	MAE	RMSE	Efficiency
x	250	250	250	250	250	0	0	0	0	100
y	162.3	162.3684	162.3684	162.3684	162.3684	0	0	0	0	100
z	104.5	104.5	104.4891	104.4991	104.5	11e-4	8.97e-4	9.37e-4	14e-4	99.999
Average						3.6e-4	2.9e-4	3.12e-4	4.66e-4	99.999

Table 5.4. Statistical Performance Evaluation of PSO-GSA

Pattern	Global	Best	Worst	Average	Median	STD	RE	MAE	RMSE	Efficiency
x	250	250	250	250	250	0	0	0	0	100
y	162.3	162.3684	162.3676	162.3682	162.3684	7.3e-4	1.77e-4	2.87e-4	7.82e-4	99.998
z	104.5	104.5	84.59	103.3	104.5	4.75	1.14	1.19	4.87	98.86
Average						1.58	0.38	0.39	1.62	99.619

Table 5.5. Statistical Performance Evaluation of GWO

Pattern	Global	Best	Worst	Average	Median	STD	RE	MAE	RMSE	Efficiency
x	250	250	250	250	250	0	0	0	0	100
y	162.3	162.3684	162.3657	162.3681	162.3684	5.17e-4	1.77e-4	2.88e-4	5.89e-4	99.998
z	104.5	104.5	104.46	104.49	104.5	6e-3	3.4e-3	36e-4	7.4e-3	99.998
Average						2.17e-3	1.19e-3	1.29e-3	2.66e-3	99.998

Table 5.6. Comparison of statistical results of PSO-GSA, GWO and BOA algorithms

Algorithm	STD	RE	MAE	RMSE	Efficiency
PSO-GSA	1.58	0.38	0.39	1.62	99.619
GWO	2.17e-3	1.19e-3	1.29e-3	2.66e-3	99.998
BOA	3.6e-4	2.9e-4	3.12e-4	4.66e-4	99.999

Table 5.7. Summary of simulation scenarios

Algorithm	Parameter	Pattern x	Pattern y	Pattern z
PSO-GSA	Min. Iteration	2	4	2
	Max. Iteration	35	51	73
	Average Iteration	12.19	16.05	21.62
	Time to GMPP	0.12	0.16	0.21
	Power	250	162.36	103.3
	Efficiency	100	99.998	98.86
GWO	Min. Iteration	2	3	2
	Max. Iteration	29	25	31
	Average Iteration	11.26	14.36	17.22
	Time to GMPP	0.11	0.14	0.07
	Power	250	162.36	104.49
	Efficiency	100	99.998	99.998
BOA	Min. Iteration	1	2	1
	Max. Iteration	25	49	52
	Average Iteration	7.37	10.13	10.28
	Time to GMPP	0.07	0.10	0.10
	Power	250	162.36	104.49
	Efficiency	100	100	99.99

It is seen from the statistical analysis that, implementing BOA decreases;

- STD by 83.41% and by 99.97%,
- RMSE by 99.97% and 82.48%,
- MAE by 99.92% and 75.81%,
- RE by 99.92% and 75.63% compared to PSO-GSA and GWO respectively.

6. CONCLUSION

In this thesis, a PV system comprising PV array, DC-DC boost converter, and the electrical load is modeled in MATLAB/Simulink and Butterfly optimization algorithm is implemented for the global optimization problem of partially shaded PV arrays that have local peaks and a global peak on its power-voltage curve. Because of its good accuracy and fast-tracking speed, a proper MPPT algorithm for the applications that have to deal with variable PSC is presented. BOA, PSO-GSA and GWO algorithms are implemented to the MPPT controller of the boost converter A comparative analysis is carried out between these MPP trackers. Three different insolation scenarios are created and three mentioned MPPT algorithms are implemented for these insolation scenarios. A comprehensive statistical analysis is also evaluated for the algorithms implemented in this study in order to compare and check the stability of the algorithms. It is seen from the statistical evaluation that implementing BOA decreases STD, RMSE, MAE, and RE and increases the efficiency compared to PSO-GSA and GWO algorithms.

According to the results it can be said that Butterfly optimization algorithm is a promising alternative for the PV systems under partial shading. A comprehensive literature summary of MPPT methods for partial shading conditions is given in chapter 2. The fundamentals of PV systems such as the structure of the PV cell, PV module and PV array are covered in Chapter 3. Chapter 4 presented the theoretical fundamentals of DC-DC converters that are implemented for the MPPT of PV systems. Detailed information about MPPT algorithms that are implemented for the PV system modeled in this thesis is also given in Chapter 4. Chapter 5 presented information about the modeled system and the simulation results. The main findings of this thesis are given below.

- The simulation results show that the modeled system by using MATLAB/Simulink comprising the PV array, DC-DC boost converter, and the load is sufficient for testing the soft computing MPPT algorithms for PV systems under partial shading conditions.
- The results show that BOA has high accuracy and the best convergence speed among the three MPPT algorithms. It is concluded from the results that for the three insolation scenarios in this study, while all the three algorithms have the same accuracy, BOA is %34,36 faster than GWO and %43.84 faster than PSO-GSA.

REFERENCES

Arora S, Singh S. 2019. Butterfly optimization algorithm: a novel approach for global optimization. Soft Computing 23: 715-734.

Baimel D, Tapuchi S, Bronshtein S, Horen Y, Baimel N. 2018. Novel Segmentation Algorithm for Maximum Power Point Tracking in PV Systems Under Partial Shading Conditions. 2018 IEEE 18th International Power Electronics and Motion Control Conference (PEMC). p. 406-410.

Barisal A, Sahu N, Prusty R, Hota P. 2012. Short-term hydrothermal scheduling using gravitational search algorithm. 2012 2nd International Conference on Power, Control and Embedded Systems. IEEE. p. 1-6.

Belhachat F, Larbes C. 2017. Global maximum power point tracking based on ANFIS approach for PV array configurations under partial shading conditions. Renewable and Sustainable Energy Reviews: 875.

Bidram A, Davoudi A, Balog RS. 2012. Control and circuit techniques to mitigate partial shading effects in photovoltaic arrays. IEEE Journal of Photovoltaics 2: 532-546.

Bosco MJ, Mabel MC. 2017. A novel cross diagonal view configuration of a PV system under partial shading condition. Solar Energy.

Choudhury S, Rout PK. 2015. Adaptive fuzzy logic based MPPT control for PV system under partial shading condition. International Journal of Renewable Energy Research 5: 1252-1263.

Davies L, Thornton R, Hudson P, Ray B. 2018. Automatic Detection and Characterization of Partial Shading in PV System. 2018 IEEE 7th World Conference on Photovoltaic Energy Conversion (WCPEC) (A Joint Conference of 45th IEEE PVSC, 28th PVSEC 34th EU PVSEC). p. 1185-1187.

Demirdelen T, Aksu IO, Esenboga B, Aygul K, Ekinci F, Bilgili M., 2019. A New Method for Generating Short-Term Power Forecasting Based on Artificial Neural Networks and Optimization Methods for Solar Photovoltaic Power Plants. In: Precup R-E, Kamal T, Zulqadar Hassan S, (eds.), Solar Photovoltaic Power Plants: Advanced Control and Optimization Techniques. Singapore: Springer Singapore. p. 165-189.

Diab AAZ, Rezk H., 2017. Global MPPT based on flower pollination and differential evolution algorithms to mitigate partial shading in building integrated PV system. Solar Energy.

Dileep G, Singh SN., 2017. An improved particle swarm optimization based maximum power point tracking algorithm for PV system operating under partial shading conditions. Solar Energy 158: 1006-1015.

El-Helw HM, Magdy A, Marei MI., 2017. A Hybrid Maximum Power Point Tracking Technique for Partially Shaded Photovoltaic Arrays. IEEE Access 5: 11900-11908.

Eltamaly AM, Farh HMH., 2019. Dynamic global maximum power point tracking of the PV systems under variant partial shading using hybrid GWO-FLC. Solar Energy: 306-316.

Javed MY, Gulzar MM, Rizvi STH, Arif A., 2016. A hybrid technique to harvest maximum power from PV systems under partial shading conditions. 2016 International Conference on Emerging Technologies (ICET). p. 1-5.

Kapić A, Zečević Ž, Krstajić B., 2018. An efficient MPPT algorithm for PV modules under partial shading and sudden change in irradiance. 2018 23rd International Scientific-Professional Conference on Information Technology (IT). p. 1-4.

Kribus A, Segev G., 2016. Solar energy conversion with photon-enhanced thermionic emission. Journal of Optics 18: 073001.

Li G, Jin Y, Akram MW, Chen X, Ji J., 2018a. Application of bio-inspired algorithms in maximum power point tracking for PV systems under partial shading conditions - A review. RENEWABLE & SUSTAINABLE ENERGY REVIEWS 81: 840-873.

Li X, Wen H, Chu G, Hu Y, Jiang L., 2018b. A novel power-increment based GMPPT algorithm for PV arrays under partial shading conditions. Solar Energy 169: 353-361.

Lyden S, Haque ME., 2016. A Simulated Annealing Global Maximum Power Point Tracking Approach for PV Modules Under Partial Shading Conditions. IEEE Transactions on Power Electronics 31: 4171-4181.

Malathy S, Ramaprabha R., 2018. A two-stage tracking algorithm for PV systems subjected to partial shading conditions. International Journal of Renewable Energy Research 8: 2249-2256.

Mangaiyarkarasi S, Raja TSR., 2014. Optimal location and sizing of multiple static var compensators for voltage risk assessment using hybrid PSO-GSA algorithm. Arabian journal for Science and Engineering 39: 7967-7980.

Manickam C, Raman GP, Raman GR, Ganesan SI, Chilakapati N., 2017. Fireworks Enriched P&O Algorithm for GMPPT and Detection of Partial Shading in PV Systems. IEEE Transactions on Power Electronics 32: 4432-4443.

Mao M, Duan Q, Duan P, Hu B., 2018. Comprehensive improvement of artificial fish swarm algorithm for global MPPT in PV system under partial shading conditions. Transactions of the Institute of Measurement & Control 40: 2178-2199.

Mao M, Duan Q, Yang Z, Duan P., 2016. Modeling and global MPPT for PV system under partial shading conditions using modified artificial fish swarm algorithm. 2016 IEEE International Symposium on Systems Engineering (ISSE). p. 1-7.

Mao M, Zhou L, Yang Z, Zhang Q, Zheng C, Xie B, Wan Y., 2019. A hybrid intelligent GMPPT algorithm for partial shading PV system. Control Engineering Practice 83: 108-115.

Martin AD, Vazquez JR, Cano JM., 2018. MPPT in PV systems under partial shading conditions using artificial vision. Electric Power Systems Research 162: 89-98.

Mirjalili S, Mirjalili SM, Lewis A., 2014. Grey wolf optimizer. Advances in engineering software 69: 46-61.

Mohamed MA, Zaki Diab AA, Rezk H., 2019. Partial shading mitigation of PV systems via different meta-heuristic techniques. Renewable Energy 130: 1159-1175.

Mohanty S, Subudhi B, Ray PK., 2016. A new MPPT design using grey wolf optimization technique for photovoltaic system under partial shading conditions. IEEE Transactions on Sustainable Energy 7: 181-188.

Mohapatra A, Nayak B, Das P, Mohanty KB., 2017. A review on MPPT techniques of PV system under partial shading condition. Renewable and Sustainable Energy Reviews: 854.

Muro C, Escobedo R, Spector L, Coppinger R., 2011. Wolf-pack (Canis lupus) hunting strategies emerge from simple rules in computational simulations. Behavioural processes 88: 192-197.

Oubbati BK, Boutoubat M, Belkheiri M, Rabhi A., 2018. Global maximum power point tracking of a PV system MPPT control under partial shading. Proceedings 2018 3rd International Conference on Electrical Sciences and Technologies in Maghreb (Cistem): 277-282.

Raizada S, Verma V., 2018. Step Up Gain Converter with fast MPPT control under moving partial shading for train rooftop PV-DC-μG. 2018 IEEE International Conference on Electrical Systems for Aircraft, Railway, Ship Propulsion and Road Vehicles International Transportation Electrification Conference (ESARS-ITEC). p. 1-6.

Ramli MAM, Ishaque K, Jawaid F, Al-Turki YA, Salam Z., 2015. A modified differential evolution based maximum power point tracker for photovoltaic system under partial shading condition. Energy & Buildings 103: 175-184.

Sameeullah M, Swarup A., 2016. MPPT Schemes for PV System under Normal and Partial Shading Condition: A Review. International Journal of Renewable Energy Development, Vol 5, Iss 2, Pp 79-94 (2016): 79.

Seyedmahmoudian M, Horan B, Soon TK, Rahmani R, Than Oo AM, Mekhilef S, Stojcevski A., 2016. State of the art artificial intelligence-based MPPT techniques for mitigating partial shading effects on PV systems – A review. Renewable and Sustainable Energy Reviews 64: 435-455.

Shang L, Zhu W, Li P, Guo H., 2018. Maximum power point tracking of PV system under partial shading conditions through flower pollination algorithm. Protection and Control of Modern Power Systems, Vol 3, Iss 1, Pp 1-7 (2018): 1.

Sundareswaran K, Vignesh kumar V, Palani S., 2015. Application of a combined particle swarm optimization and perturb and observe method for MPPT in PV systems under partial shading conditions. Renewable Energy 75: 308-317.

Tey KS, Mekhilef S, Seyedmahmoudian M, Horan B, Oo AT, Stojcevski A., 2018. Improved Differential Evolution-Based MPPT Algorithm Using SEPIC for PV Systems Under Partial Shading Conditions and Load Variation. IEEE Transactions on Industrial Informatics 14: 4322-4333.

Yang B, Yu T, Zhang X, Li H, Shu H, Sang Y, Jiang L., 2019a. Dynamic leader based collective intelligence for maximum power point tracking of PV systems affected by partial shading condition. Energy Conversion and Management 179: 286-303.

Yang B, Zhong L, Shu H, Zhang X, Yu T, Li H, Jiang L, Sun L., 2019b. Novel bio-inspired memetic salp swarm algorithm and application to MPPT for PV systems considering partial shading condition. Journal of Cleaner Production 215: 1203-1222.

BIOGRAPHY

Kemal AYGÜL was born in Adana, Turkey in 1994. He received his B.Sc. degree in Department of Electrical and Electronics Engineering of Çukurova University in 2016. After his graduation from B.Sc. degree he started his master of science degree in Department of Electrical and Electronics Engineering of Çukurova University also. He has been working as a Research Assistant in the same department since 2018. His research areas are Renewable Energy Technologies and Electric Machines.